https://doi.org/10.5194/egusphere-2022-1154
Preprint. Discussion started: 9 December 2022

Ozone–NO_x–VOC Sensitivity of the Lake Michigan Region Inferred from TROPOMI Observations and Ground-Based Measurements

J. Jerrold M. Acdan[1*], R. Bradley Pierce[1,2], Angela F. Dickens[3], Zachariah Adelman[3], Tsengel Nergui[3]

[1]Department of Atmospheric and Oceanic Sciences, University of Wisconsin-Madison, Madison, WI, 53706, United States
[2]Space Science and Engineering Center, University of Wisconsin-Madison, Madison, WI, 53706, United States
[3]Lake Michigan Air Directors Consortium (LADCO), Hillside, IL, 60162, United States

Correspondence to: J. Jerrold M. Acdan (acdan@wisc.edu)

Abstract. Surface-level ozone (O_3) is a secondary air pollutant that has adverse effects on human health. In the troposphere, O_3 is produced in complex cycles of photochemical reactions involving nitrogen oxides (NO_x) and volatile organic compounds (VOCs). Determining if O_3 production will be decreased by lowering NO_x emissions ("NO_x-sensitive"), VOC emissions ("VOC-sensitive"), or both ("the transition zone") can be done by using the formaldehyde (HCHO; a VOC species) to nitrogen dioxide (NO_2; a component of NO_x) concentration ratio ([HCHO]/[NO_2]; "FNR"). Generally, lower FNR values indicate VOC sensitivity while higher values indicate NO_x sensitivity. In this study, we use FNRs calculated from 2019–2021 TROPOspheric Monitoring Instrument (TROPOMI) satellite data and 2019 Photochemical Assessment Monitoring Station (PAMS) ground-based data to investigate the ozone–NO_x–VOC sensitivity of the Lake Michigan region, an area that regularly exceeds the United States Environmental Protection Agency's regulatory standards for O_3. We find that TROPOMI FNRs are always greater than PAMS FNRs, indicating that they must be interpreted with different threshold values to infer O_3 chemistry sensitivities. Further analysis of TROPOMI FNRs reveals that during both typical O_3 season days and Chicago, Illinois, O_3 exceedance days, the average O_3 chemistry sensitivity is: (1) VOC-sensitive in the Chicago metropolitan area (CMA), (2) transitional in the areas surrounding the CMA and up the western Lake Michigan coastline to Milwaukee, Wisconsin, and (3) NO_x-sensitive in the rest of the domain. However, the magnitude of FNR values change during exceedance days, indicating that areas that are NO_x-sensitive (VOC-sensitive) during typical O_3 season days increase in NO_x-sensitivity (VOC-sensitivity). Additionally, the transition zone area decreases by 25% on exceedance days. Comparing weekends to weekdays, O_3 chemistry in the Chicago metropolitan area becomes more NO_x-sensitive on weekends due lower NO_x emissions. Finally, analysed 10-meter wind data shows that the lake breeze circulation, which transports high O_3 levels from over Lake Michigan to onshore coastal areas, is stronger during O_3 exceedance days compared to typical O_3 season days, and there are no major weekday-weekend differences in the properties of the 10-meter wind field.

https://doi.org/10.5194/egusphere-2022-1154
Preprint. Discussion started: 9 December 2022

1 Introduction

Ground-level ozone (O_3) is an air pollutant that is known for its harmful effects on public health. Exposure to elevated O_3 levels can cause acute respiratory problems and lead to premature death from respiratory and circulatory system illnesses over longer timescales (Jerrett et al., 2009; Turner et al., 2016; Nuvolone et al., 2018). To prevent such adverse effects, the United States Environmental Protection Agency (U.S. EPA) sets a National Ambient Air Quality Standard (NAAQS) for O_3, which is currently 70 parts per billion by volume (ppbv) for the fourth-highest daily maximum 8-hour concentration (MDA8), averaged across three consecutive years (U.S. EPA, 2022a). The U.S. EPA designates counties in the U.S. where O_3 concentrations exceed the O_3 NAAQS as O_3 nonattainment areas (NAAs), and these areas are required by law to develop State Implementation Plans (SIPs) to address the problem. One such region of the U.S. that continues to be in violation of the O_3 NAAQS is the Lake Michigan region, including NAAs in the states of Illinois, Indiana, Michigan, and Wisconsin (U.S. EPA, 2022b).

Developing strategies to decrease surface O_3 levels is complicated because O_3 is a secondary pollutant not directly emitted into the atmosphere. Many studies have shown that the production rate of tropospheric O_3 is a non-linear function of the concentrations of the precursor species nitrogen oxides (NO_x) and volatile organic compounds (VOCs) (Haagen-Smit, 1952; Milford et al., 1989; Sillman, 1995). In the Lake Michigan region, NO_x emissions primarily come from anthropogenic fossil fuel combustion, such as diesel and gasoline vehicle usage, electricity generation, and industrial processes (U.S. EPA, 2021). VOC emissions come from both anthropogenic sources (e.g., paint and solvent application) and natural biogenic emissions from plants and crops (U.S. EPA, 2021). Further details about the chemical cycles involving NO_x and VOCs that produce tropospheric O_3 can be found in Jacob (1999, 2000), Thornton et al. (2002), Schroeder et al. (2017), and Vermeuel et al. (2019).

Despite the complexities of surface O_3 production, O_3 formation can be generally classified into two primary chemistry regimes: VOC-sensitive and NO_x-sensitive. In the VOC-sensitive regime, VOC emissions reductions decrease organic radical (RO_2) formation, which then leads to less cycling with NO_x and thus less O_3 formation (Milford et al., 1989; Jin and Holloway, 2015). Conversely, reductions in NO_x emissions in the VOC-sensitive regime can lead to increased O_3 formation due to non-linearities in the O_3 chemistry. In the NO_x-sensitive regime, NO_x emissions reductions decrease the amount of NO_2 available for photolysis, thus reducing the amount of free oxygen atoms that are available to combine with oxygen molecules (O_2) to form O_3 (Jin and Holloway, 2015). In a third regime between VOC and NO_x sensitivities ("the transition zone"), O_3 production can be reduced by decreasing either or both VOC and NO_x emissions (Jin and Holloway, 2015). Therefore, knowing the O_3 chemistry sensitivity within a geographical area is informative for regulatory agencies responsible for developing O_3 NAAQS attainment strategies through NO_x and VOC emissions control programs.

https://doi.org/10.5194/egusphere-2022-1154
Preprint. Discussion started: 9 December 2022

One of the ways O_3 chemistry sensitivities can be identified is through indicator ratios. Sillman (1995) found that the formaldehyde (HCHO) to reactive nitrogen (NO_y) concentration ratio ([HCHO]/[NO_y]) is a viable indicator for ozone–NO_x–VOC sensitivity. HCHO can be used as a proxy for VOC concentrations because many VOC oxidation reactions in O_3 chemistry cycles produce HCHO (Sillman, 1995; Valin et al., 2016). Building upon Sillman's work, Tonnesen and Dennis (2000) found that the formaldehyde to nitrogen dioxide concentration ratio ([HCHO]/[NO_2]; referred to as "FNR" for the rest of this paper) is a more useful indicator of ozone–NO_x–VOC sensitivity since HCHO and NO_2 have similar lifetimes (on the order of hours) while NO_y has a lifetime on the order of days. Using species with similar lifetimes in the indicator ratio better represents the interactions between the catalytic cycles that result in O_3 production (Tonnesen and Dennis, 2000).

The FNR indicator ratio is well-suited for satellite data analyses because HCHO and NO_2 column densities are both measurable from space. Satellite-derived FNRs from the Global Ozone Monitoring Experiment (GOME), SCanning Imaging Absorption spectroMeter for Atmospheric CartograpHY (SCIAMACHY), and Ozone Monitoring Instrument (OMI) have been used to infer ozone–NO_x–VOC sensitivity for many regions around the world (Martin et al., 2004; Duncan et al., 2010; Jin and Holloway, 2015; Chang et al., 2016; Jin et al., 2017; Jin et al., 2020). Despite being applied in many analyses, the threshold FNR values used to distinguish between VOC-sensitive and NO_x-sensitive O_3 chemistry varies by study. Much of the early work in this line of research (e.g., Martin et al., 2004; Duncan et al., 2010) used models to estimate FNR threshold values. However, model results can be biased due to errors in input datasets or imperfect representations of physical processes within the models themselves (Brown-Steiner et al., 2015). A more recent study by Jin et al. (2020; referred to as "J20" for the rest of this work) avoids model biases by connecting satellite data directly to ground monitor data to estimate FNR threshold values for major cities in the U.S., including Chicago, Illinois, in the Lake Michigan region. **Table 1** displays the J20 threshold values for different O_3 chemistry sensitivities.

Table 1: J20 FNR threshold values indicating different O_3 chemistry sensitivities for Chicago, Illinois, U.S.

Source	VOC-sensitive	Transition zone	NO_x-sensitive
Jin et al. 2020 ("J20")	FNR < 3.2	3.2 < FNR < 4.1	FNR > 4.1

In this work, we apply the J20 O_3 chemistry sensitivity thresholds to satellite FNRs to assess the average 2019-2021 spatial distribution of ozone–NO_x–VOC sensitivity in the Lake Michigan region. We calculate FNR values using retrievals from the TROPOspheric Monitoring Instrument (TROPOMI) onboard the Sentinel-5 Precursor (S5P) satellite as well as ground-based measurements from a Photochemical Assessment Monitoring Station (PAMS). After comparing the satellite-based and ground-based FNR values, we further analyse the satellite FNRs to compare typical O_3 season days to O_3 exceedance days and weekdays to weekends. We supplement these investigations with an analysis of 10-meter winds to provide meteorological context to the satellite-based results.

https://doi.org/10.5194/egusphere-2022-1154
Preprint. Discussion started: 9 December 2022

2 Data & methodology

2.1 Satellite data: S5P TROPOMI

The S5P satellite was launched in October 2017 and has a polar, sun-synchronous orbit, providing global daily data approximately at 13:30 local solar time (Ludewig et al., 2020). TROPOMI is an ultraviolet-visible-near infrared-shortwave infrared nadir-viewing grating spectrometer onboard the S5P satellite that measures trace gases in the atmosphere as well as cloud and aerosol properties (Veefkind et al., 2012; van Geffen et al., 2020). The original spatial resolution of TROPOMI data was 3.5 km x 7 km. Since August 2019, the spatial resolution has been upgraded to 3.5 km x 5.5 km (van Geffen et al., 2020). TROPOMI retrievals have signal-to-noise ratios (SNRs) that are similar to the Ozone Monitoring Instrument (OMI) but with much higher spatial resolution (Veefkind et al., 2012; De Smedt et al., 2018). To calculate satellite FNRs, we downloaded S5P TROPOMI version 1 and 2 tropospheric NO_2 (Koninklijk Nederlands Meteorologisch Instituut [KNMI], 2018, 2019, 2021) and tropospheric HCHO (German Aerospace Center [DLR], 2019, 2020) orbital level 2 (L2) data for the O_3 seasons of 2019, 2020, and 2021 from the NASA Goddard Earth Sciences Data and Information Services Center (GES DISC). We define May to September as the O_3 season because this is the period in which most O_3 exceedance days occur in Chicago, Illinois, which is the area that experiences the most exceedances in the Lake Michigan region (**Appendix Table A1**). An O_3 exceedance day is defined as a day in which at least one ground monitor measures MDA8 O_3 levels above the U.S. EPA O_3 NAAQS (70 ppbv).

Details regarding the TROPOMI NO_2 tropospheric vertical column retrieval algorithm are found in van Geffen et al. (2021). The total uncertainty in NO_2 tropospheric vertical column density retrievals is estimated to be between 15–50 % for larger columns over continental areas (Boersma et al., 2018; van Geffen et al., 2021). Version 1 of TROPOMI NO_2 tropospheric column data had an average bias of -32 % while version 2 had an average bias of -23 % (i.e., are 32 % and 23 % too low, respectively) when compared to ground-based tropospheric column measurements (van Geffen et al., 2022). Specifics regarding the TROPOMI HCHO tropospheric vertical column retrieval algorithm are found in De Smedt et al. (2018). The total uncertainty in HCHO tropospheric vertical column density retrievals is currently estimated to be between 30–60 % in polluted conditions, including random and systematic slant column contributions (De Smedt et al., 2021). TROPOMI HCHO data are systematically biased by approximately -25 % (i.e., are 25 % too low) for HCHO columns larger than 8 x 10^{15} molecules per square centimeter (mol cm^{-2}) when compared to ground-based column measurements (De Smedt et al., 2021). If the uncertainties in TROPOMI HCHO and NO_2 retrievals are uncorrelated, the combined uncertainty in the [HCHO]/[NO_2] ratio is between 34–78 % (see **Appendix B** for calculation). However, Martin et al. (2004) and Duncan et al. (2010) note that uncertainties from air mass factor calculations (due to clouds, albedo, background corrections, etc.) affect both HCHO and NO_2 retrievals, so these types of errors are likely correlated and tend to cancel out in the [HCHO]/[NO_2] ratio. Thus, 34–78 % should be taken as an upper limit for the uncertainty of FNRs presented in this work.

https://doi.org/10.5194/egusphere-2022-1154
Preprint. Discussion started: 9 December 2022

2.1.1 Satellite data processing: S5P TROPOMI composites

TROPOMI retrievals of HCHO are primarily derived from the instrument's spectral Band 3 (range: 310–405 nm), while NO_2 retrievals are derived from spectral Band 4 (range: 405–500 nm) (Veefkind et al., 2012; De Smedt et al., 2018; van Geffen et al., 2021). Both bands have a minimum signal-to-noise ratio (SNR) between 800 and 1000 (Veefkind et al., 2012). However, HCHO has an optical density that is an order of magnitude smaller than that of NO_2, resulting in HCHO retrievals with lower SNRs than NO_2 retrievals (De Smedt et al., 2018). Despite lower SNRs in individual retrievals, Vigouroux et al. (2020) found that monthly mean TROPOMI HCHO composites correlate well with ground-based Fourier-transform infrared (FTIR) station measurements of HCHO vertical column densities, verifying that the precision of TROPOMI measurements allow the seasonal variability in HCHO levels to be well captured. To reduce the impacts of lower SNRs of TROPOMI HCHO retrievals and to allow for the analysis of general spatial patterns in FNR values, we composited TROPOMI HCHO and NO_2 data on monthly and seasonal timescales. We constructed gridded mean TROPOMI HCHO and NO_2 'clear sky' (cloud radiance fraction < 0.5) composites using quality controlled L2 retrievals based on the recommended qa_value > 0.75 for HCHO (De Smedt et al., 2022) and NO_2 (Eskes and Eichmann, 2021). Additional detection limit filters of 1.8×10^{15} mol cm^{-2} for HCHO (Chance, 2002) and 1.5×10^{15} mol cm^{-2} for NO_2 (Duncan et al., 2010) were applied to the L2 orbital retrievals used in the composites. It is important to note that these detection limit values are for OMI data, but it is assumed that the same values can be applied to TROPOMI data because both instruments have similar signal-to-noise ratios.

https://doi.org/10.5194/egusphere-2022-1154
Preprint. Discussion started: 9 December 2022

The grid onto which the TROPOMI data were composited has a spatial resolution of 12 km x 12 km covering the continental United States with a Lambert Conformal Conic projection. We spatially subset the composites to the Lake Michigan region (latitude bounds: 41 °N to 45.3 °N; longitude bounds: 88.6 °W to 85.49 °W) for analysis (**Fig. 1**).

Figure 1: Map of the Lake Michigan region with the study area highlighted in orange. The locations of cities mentioned in this work are denoted with a black dot.

We produced TROPOMI HCHO and NO_2 composites for four distinct categories: (1) typical O_3 season days, (2) O_3 exceedance days, (3) weekdays, and (4) weekends (**Table 2**). To create a "typical O_3 season day composite", we first created monthly average composites for May to September for the years 2019, 2020, and 2021. We then combined the resulting 15 individual composites by taking the weighted averages of the monthly composites (based on the number of observations per grid cell) to get an overall 2019–2021 typical O_3 season day composite. Next, we next created an "O_3 exceedance day composite" by compositing satellite data only on days in which at least one ground monitor in the U.S. EPA Air Quality System (AQS) within the Chicago, Illinois, metropolitan area measured an MDA8 O_3 value greater than the NAAQS 70 ppbv standard. For this composite, we deemed Chicago, Illinois, as representative of the Lake Michigan domain since it is the area that experiences the most O_3 exceedances in the region. Therefore, the exceedance day composite included 53 days of TROPOMI data (**Appendix Table A1**). We also created weekday and weekend composites following a similar procedure as that for the O_3 season by first compositing weekday and weekend data for individual years and then taking the weighted average to get overall 2019–2021 weekday and weekend composites. For each composite category, we constructed FNR composites by dividing the

https://doi.org/10.5194/egusphere-2022-1154
Preprint. Discussion started: 9 December 2022

composite weighted average HCHO and NO_2 values for each grid cell. The resulting FNR composites were then analysed using the J20 threshold values to infer O_3 chemistry sensitivities.

Table 2: Categories of TROPOMI data composites created in this study.

Composite category	Amount of data composited
Ozone season (May to September)	459 days (15 months)
Chicago O_3 exceedance days	53 days
Weekdays	327 days
Weekends	132 days

To provide meteorological context to the FNR analyses, we also composited 10-meter height east-west (U) and north-south (V) winds that are available at each TROPOMI pixel within the downloaded TROPOMI data files. These wind data originally come from the European Centre for Medium-Range Weather Forecasts (ECMWF) analysis (Eskes et al., 2021). In addition to wind speed and direction, we also calculated and analysed the divergence of the composited wind field (units: s^{-1}) via fourth order approximations of the horizontal derivatives of U and V (**Eq. 1**–**3**; adapted from Kalnay-Rivas and Hoitsma, 1979):

$$\nabla \cdot \vec{V} = \frac{\partial U}{\partial x} + \frac{\partial V}{\partial y} \quad \textbf{(1)}$$

$$\frac{\partial U}{\partial x} = \frac{4}{3}\left(\frac{U(x+\Delta x)-U(x-\Delta x)}{2\Delta x}\right) - \frac{1}{3}\left(\frac{U(x+2\Delta x)-U(x-2\Delta x)}{4\Delta x}\right) \quad \textbf{(2)}$$

$$\frac{\partial V}{\partial y} = \frac{4}{3}\left(\frac{V(y+\Delta y)-V(y-\Delta y)}{2\Delta y}\right) - \frac{1}{3}\left(\frac{V(y+2\Delta y)-V(y-2\Delta y)}{4\Delta y}\right) \quad \textbf{(3)}$$

2.2 Ground data & processing: PAMS monitoring site

To provide further context to TROPOMI-based FNRs, we also calculated FNRs from ground-based data. We obtained Photochemical Assessment Monitoring Station (PAMS) data for the year 2019, which contains surface HCHO and NO_2 measurements for various sites across the U.S. To compare surface FNRs to the satellite FNRs, we considered only sites within the Lake Michigan domain that reported concurrent HCHO and NO_2 measurements during the O_3 season. This resulted in a single PAMS location for analysis: Site 3103 in Schiller Park, Cook County, Illinois (41.965 ºN, 87.876 ºW). The location of this PAMS site is adjacent to the Chicago O'Hare International airport and major highways.

https://doi.org/10.5194/egusphere-2022-1154
Preprint. Discussion started: 9 December 2022

At this site, HCHO measurements were taken every 6 days in 24-hour sampling intervals while NO_2 measurements were taken every day in 1-hour intervals. To process the data, we first converted the HCHO data from their original units of micrograms per cubic meter ($\mu g/m^3$) to the same units as the NO_2 data (ppb) assuming standard pressure and temperature (because measured pressure and temperature were not available in the downloaded PAMS dataset). Next, we filtered the NO_2 data to include only the days with concurrent HCHO measurements. These values were then averaged to get individual monthly HCHO and NO_2 values. The monthly values were then divided to get monthly FNR values to compare them to the previously generated monthly composites of TROPOMI data. All available data were used to calculate monthly means for both TROPOMI and PAMS FNR values (i.e., the TROPOMI FNR composites used in the comparison were not subsampled to include only days in which PAMS data were available).

https://doi.org/10.5194/egusphere-2022-1154
Preprint. Discussion started: 9 December 2022

3 Results & discussion

3.1 Comparison of TROPOMI satellite-based and PAMS ground-based FNRs

Figure 2a is a time series plot of HCHO and NO_2 ground measurements at PAMS Site 3103 in Schiller Park, Illinois, during the 2019 O_3 season. The orange dots represent the 24-hour samples of HCHO, sampled every sixth day, while the smaller blue dots indicate the hourly NO_2 measurements on those days. The larger blue dots are the daily average of the hourly NO_2 measurements, which show that a significant amount of variability is lost when averaging over 24-hour timescales. Since both NO_2 and HCHO photolysis follow similar diurnal cycles (Ruiz-Suarez et al., 1993), 24-hour sampling also obscures the fluctuations in atmospheric HCHO levels that occur on shorter timescales. **Figure 2b** displays the monthly mean of the data plotted in **Figure 2a**. Monthly mean NO_2 levels are greater than HCHO levels for all months during the 2019 O_3 season. **Figure 2c** shows a time series comparison between the PAMS ground-based and TROPOMI satellite-derived composite FNR values at Schiller Park, Illinois. All ground-based monthly FNR values are less than 1, ranging from a minimum of 0.25 (May) to a maximum of 0.68 (July). For all months, the TROPOMI FNR values (ranging from a minimum of 1.76 [May] to a maximum of 2.87 [August]) are greater than the PAMS FNR values.

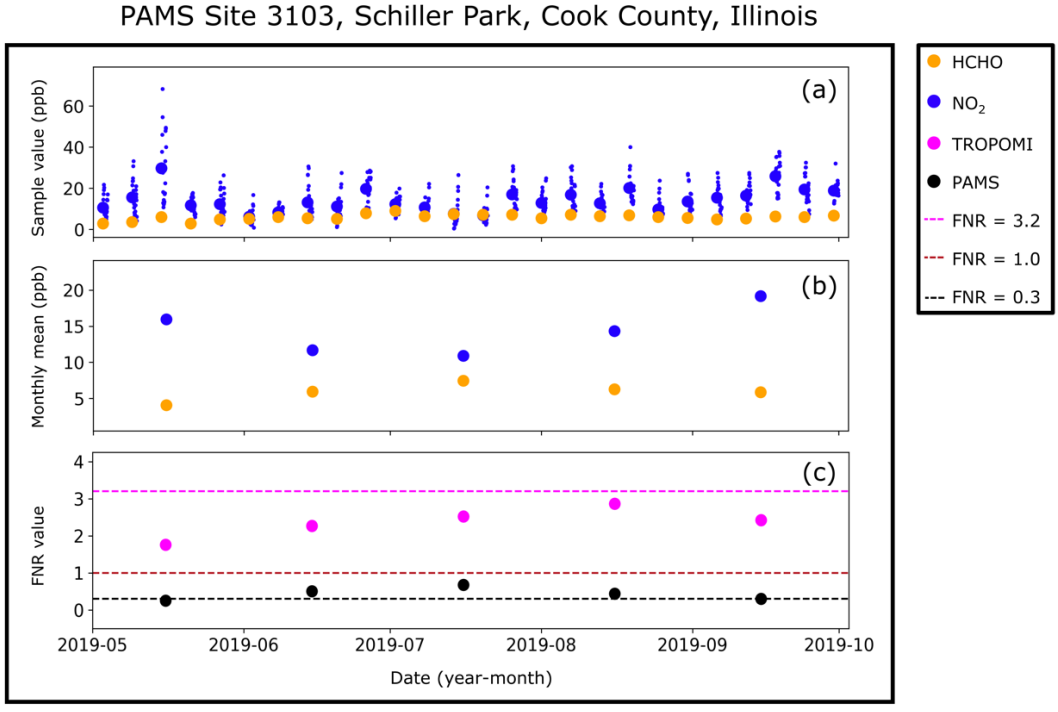

Figure 2: (a) HCHO (orange) and NO_2 (blue) PAMS surface measurements, (b) monthly averaged HCHO (orange) and NO_2 (blue) PAMS values, and (c) FNRs calculated from PAMS measurements (black) and TROPOMI retrievals (pink). Areas beneath the dashed pink and black lines represent FNRs indicating VOC-sensitive O_3 chemistry based on the Jin et al. (2020) and Blanchard (2020) studies, respectively. The area between the dashed brown and black lines represents FNRs indicating transitional O_3 chemistry based on Blanchard (2020).

https://doi.org/10.5194/egusphere-2022-1154
Preprint. Discussion started: 9 December 2022

The discrepancy between the PAMS and TROPOMI FNR values could be due to many factors including, but not limited to: (1) the relatively long PAMS HCHO and NO_2 sampling duration compared to the instantaneous TROPOMI sampling at 13:30 local time (near the time of peak FNR values; Blanchard, 2020), (2) vertical profile differences between HCHO and NO_2 that make surface values that PAMS measures different than tropospheric column values that TROPOMI measures (Schroeder et al., 2017), and (3) high biases in monitored NO_2 due to the use of a nonselective detector (Blanchard, 2020). Regardless, this analysis shows that different sets of O_3 chemistry sensitivity threshold values must be used to interpret ground-based and satellite-based FNRs. A study by Blanchard (2020) argues that the FNR value indicating the transition between VOC-sensitive and NO_x-sensitive O_3 chemistry lies between ~0.3–1.0 for the Lake Michigan region. The argument is based on: (1) the transitional O_3 chemistry FNR thresholds found in previous studies (e.g., 0.8–1.8 in Tonnesen and Dennis [2000]; 1–2 in Duncan et al. [2010]; 0.7–2.3 in Schroeder et al. [2017]; and 3.2–4.1 in Jin et al. [2020]), (2) the reasons listed above for discrepancies between PAMS and TROPOMI FNRs, and (3) original analyses of surface observations in the Lake Michigan region. If we apply the Blanchard (2020) thresholds to the surface FNRs calculated using PAMS data, we see that O_3 production was VOC-sensitive in May and September and transitional in June, July, and August in 2019 at this PAMS site.

The J20 thresholds were derived by connecting satellite-derived FNRs to high O_3 event probabilities calculated from ground monitor data. Therefore, the J20 thresholds are well suited to interpret TROPOMI-derived FNRs. If we apply the J20 thresholds to the TROPOMI data, we see that O_3 production at this PAMS site is VOC-sensitive for the entire study period in 2019. Comparisons between the ground-based and satellite-based FNRs indicate different O_3 chemistry sensitivities from June to August (transitional versus VOC-sensitive, respectively). However, there is some uncertainty with the true lower end value of the Blanchard (2020) transitional O_3 chemistry FNR threshold range (~0.3–1.0). If the true lower end value were greater, such as 0.7 reported by Schroeder et al. (2017), then the PAMS FNRs would also indicate that O_3 production is VOC-sensitive at this site for the entire study period in 2019.

https://doi.org/10.5194/egusphere-2022-1154
Preprint. Discussion started: 9 December 2022

3.2 Comparison of O_3 season and O_3 exceedance day TROPOMI composites

Figure 3 displays composite mean NO_2 levels derived from TROPOMI data during the ozone season ('OS'; **Fig. 3a**) and Chicago ozone exceedance days ('Ex'; **Fig. 3b**), along with mean 10-meter wind vectors. During the ozone season, mean NO_2 levels range from 1.95 x 10^{15} to 5.69 x 10^{15} mol cm^{-2}, with a regional average of 2.44 x 10^{15} mol cm^{-2}. During Chicago exceedance days, mean NO_2 levels range from 1.84 x 10^{15} to 7.60 x 10^{15} mol cm^{-2}, with a regional average of 2.51 x 10^{15} mol cm^{-2}. Additional statistics for these composites can be found in **Appendix Table C1**. The spatial distribution of NO_2 levels in both composites shows a clear hotspot of emissions in the Chicago, Illinois, metropolitan area (CMA). **Figure 3c**, the difference between the exceedance day and ozone season composites, shows that mean NO_2 levels are higher in the CMA and north along the western Lake Michigan coastline during exceedance days, with the greatest increase of 1.91 x 10^{15} mol cm^{-2} in the urban core of Chicago. Further research is needed to investigate reasons why NO_2 levels are higher in the CMA during Chicago O_3 exceedance days.

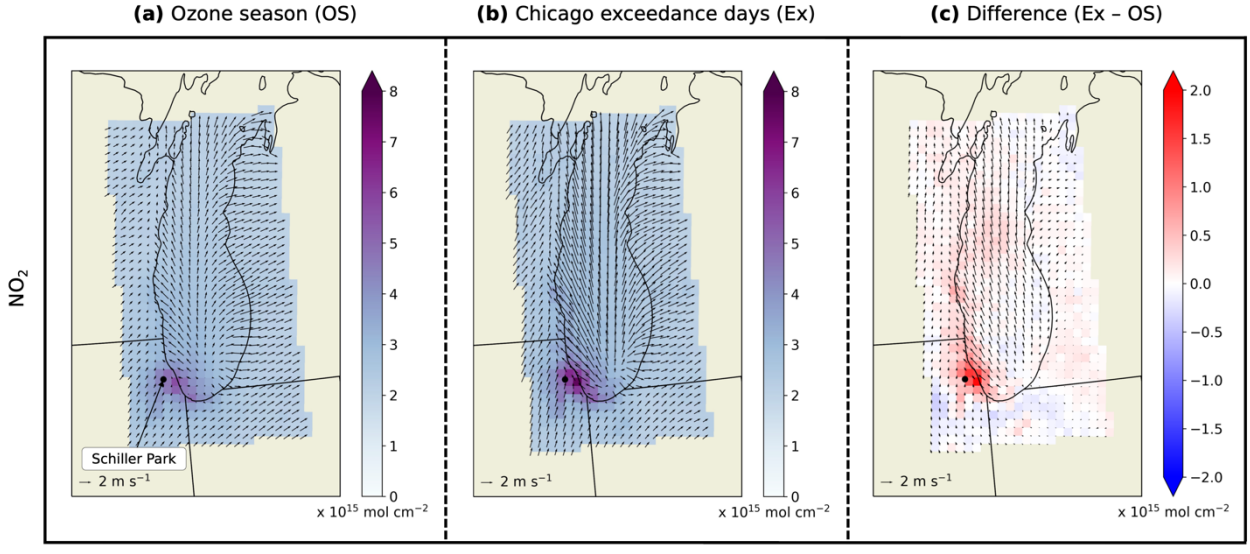

Figure 3: TROPOMI-derived composites of 2019–2021 mean tropospheric NO_2 in the Lake Michigan region during: (a) the ozone season (OS), (b) Chicago ozone exceedance days (Ex), and (c) the difference between them (Ex – OS). Mean 10-meter winds are represented by arrows.

https://doi.org/10.5194/egusphere-2022-1154
Preprint. Discussion started: 9 December 2022

Figure 4 displays composite mean HCHO levels derived from TROPOMI data during the ozone season (**Fig. 4a**) and Chicago exceedance days (**Fig. 4b**), along with mean 10-meter wind vectors. During the ozone season, mean HCHO levels range from 10.2 x 10^{15} to 13.8 x 10^{15} mol cm^{-2}, with a regional average of 11.9 x 10^{15} mol cm^{-2}. During Chicago exceedance days, mean HCHO levels range from 9.64 x 10^{15} to 16.2 x 10^{15} mol cm^{-2}, with a regional average of 13.0 x 10^{15} mol cm^{-2}. Additional statistics for these composites can be found in **Appendix Table C1**. In general, the spatial distribution of HCHO in both composites is relatively homogeneous (compared to NO_2), though higher levels can be seen over the southern part of the lake and along the eastern Lake Michigan coastline. **Figure 4c**, the difference between the Chicago exceedance day and ozone season composites, shows that mean HCHO levels are higher during Chicago ozone exceedance days, with an average regional increase of 1.13 x 10^{15} mol cm^{-2}. Because positive differences occur over the entire domain (as opposed to occurring in localized hotspots), the higher HCHO abundances are likely due to increased temperatures during O_3 exceedance events, which lead to increased biogenic VOC emissions and thus increased O_3 production (Sillman and Samson, 1995).

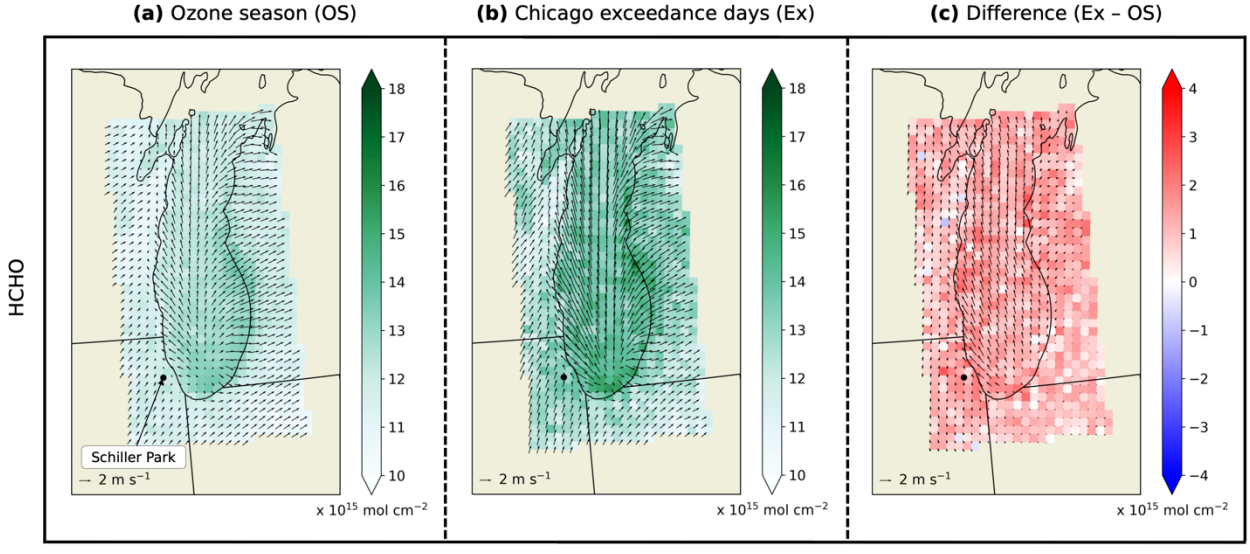

Figure 4: TROPOMI-derived composites of 2019–2021 mean tropospheric HCHO in the Lake Michigan region during: (a) the ozone season (OS), (b) Chicago ozone exceedance days (Ex), and (c) the difference between them (Ex – OS). Mean 10-meter winds are represented by arrows.

https://doi.org/10.5194/egusphere-2022-1154
Preprint. Discussion started: 9 December 2022

Figure 5 displays composite mean FNR values during the ozone season (**Fig. 5a**) and Chicago exceedance days (**Fig. 5b**), along with mean 10-meter wind vectors. During the ozone season, mean FNR values range from 2.12 to 6.12, with a regional average of 4.99. During Chicago exceedance days, mean FNR values range from 1.84 to 7.11, with a regional average of 5.34. Additional statistics for these composites can be found in **Appendix Table C1**. In both composites, the lowest FNR values occur in the CMA, its surroundings, and north along the eastern Illinois and Wisconsin shorelines. The highest values are found along the western Michigan shoreline. **Figure 5c**, the difference between the Chicago exceedance day and ozone season composites, shows that mean FNR values are lower in the urban core of Chicago and in some parts north along the western Lake Michigan coastline during exceedance days, indicating more VOC-sensitive O_3 chemistry relative to all days across the season. However, for most of the region, mean FNR values are higher on exceedance days (with a regional average increase of 1.54), indicating increasingly NO_x-sensitive O_3 chemistry.

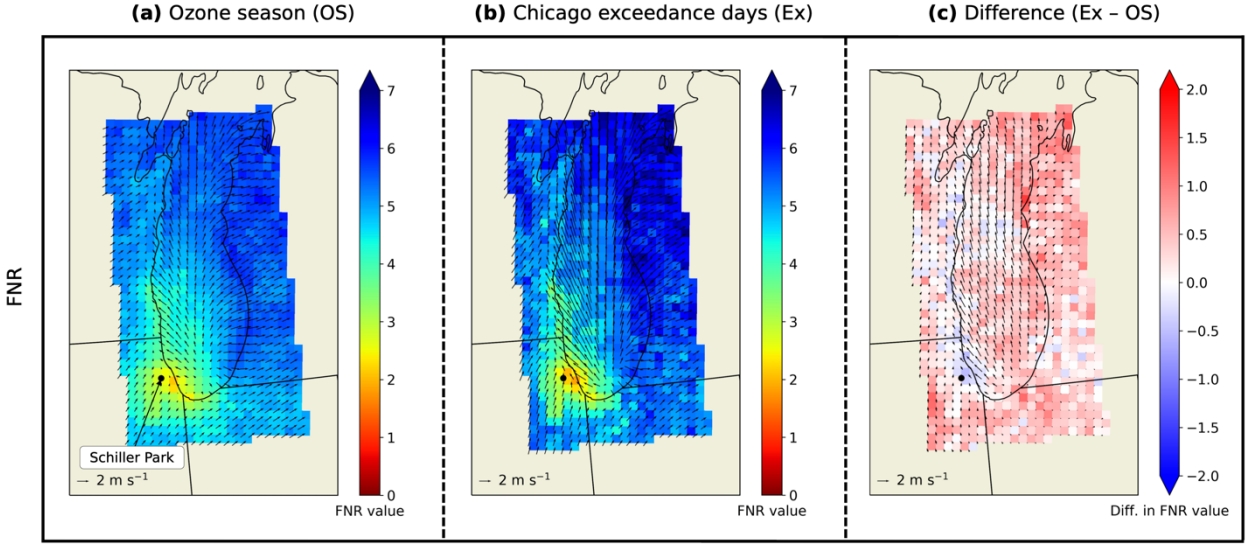

Figure 5: TROPOMI-derived 2019–2021 FNR values in the Lake Michigan region during: (a) the ozone season (OS), (b) Chicago ozone exceedance days (Ex), and (c) the difference between them (Ex – OS). Mean 10-meter winds are represented by arrows.

https://doi.org/10.5194/egusphere-2022-1154
Preprint. Discussion started: 9 December 2022

When the mean FNR values are interpreted using the J20 thresholds, we see similar spatial distributions of O_3 chemistry sensitivities between typical ozone season days (**Fig. 6a**) and Chicago exceedance days (**Fig. 6b**). For both composites, the Chicago metropolitan area is VOC-sensitive, while its surroundings and north along the western shoreline of Lake Michigan up to Milwaukee are in the transition zone between VOC and NO_x sensitivities. The rest of the domain is NO_x-sensitive. The spatial distributions of O_3 chemistry sensitivities are similar for two reasons: (1) higher NO_2 levels in Chicago during exceedance days counterbalances higher regional HCHO concentrations, thus making the Chicago metropolitan area remain VOC-sensitive (note that the urban core of Chicago becomes even more VOC-sensitive as indicated by decreases in FNR values seen in **Fig.5c**), and (2) the largest increases in FNR values (indicating increasing NO_x sensitivity) are outside of Chicago in the regions that are already NO_x-sensitive. It is interesting to note that the area classified as having transitional chemistry changes from 7.3 % during the ozone season to 5.5 % on Chicago exceedance days, which is a decrease in value of 25 %. This is due to increased HCHO levels that shift transition zone areas in the ozone season composite to NO_x-sensitive areas in the exceedance day composite.

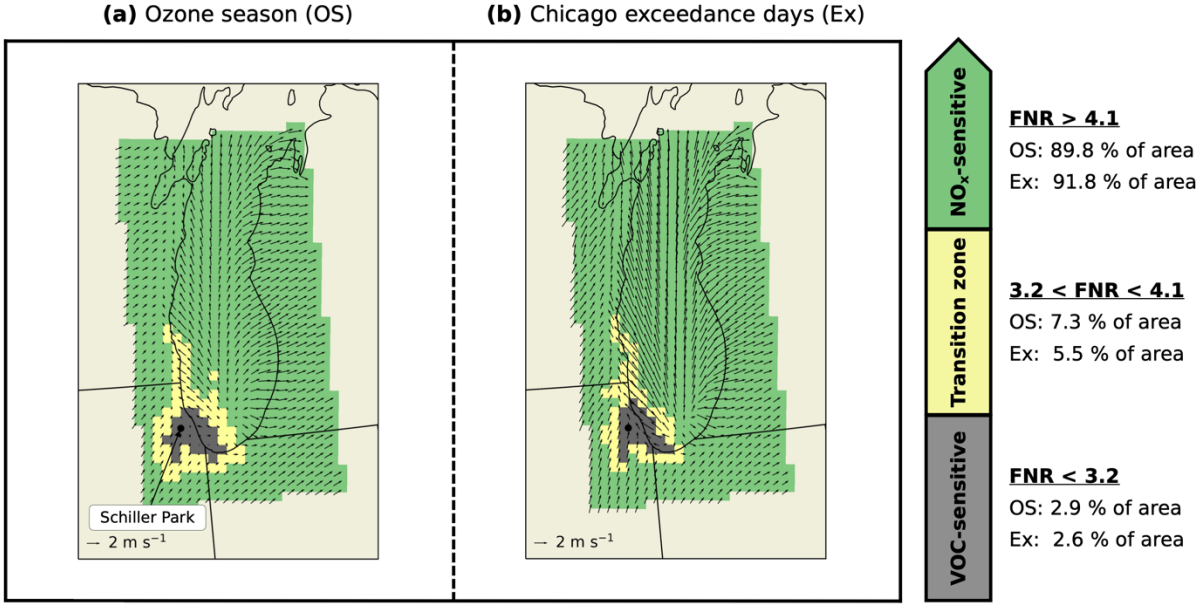

Figure 6: J20 threshold interpretation of 2019–2021 ozone–NO_x–VOC sensitivity in the Lake Michigan region during: (a) the ozone season and (b) Chicago ozone exceedance days. Mean 10-meter winds are represented by arrows.

These results are similar to those of Vermeuel et al. (2019) and Acdan et al. (2020), who used chemical box modeling to investigate the O_3 production sensitivity of air parcels as they traveled on O_3 exceedance days (June 2/4/11/12/15, 2017) from their Chicago-Gary (Illinois-Indiana) urban source regions to over Lake Michigan, and then north along the coast to the border between Illinois and Wisconsin. Their findings show that O_3 production within the plumes transitioned from having more

https://doi.org/10.5194/egusphere-2022-1154
Preprint. Discussion started: 9 December 2022

365 VOC-sensitive O_3 chemistry in the Chicago-Gary urban source regions to having more NO_x-sensitive O_3 chemistry as they advected north along the Lake Michigan coastline. Our results and those of Vermeuel et al. (2019) and Acdan et al. (2020) find a general south-north gradient in O_3 chemistry that transitions toward less VOC sensitivity/more NO_x sensitivity starting from the south in the Chicago metropolitan area and going north along the western Lake Michigan shoreline.

370

375

380

385

390

395

https://doi.org/10.5194/egusphere-2022-1154
Preprint. Discussion started: 9 December 2022

Figure 7 displays plots of mean 10-meter wind vectors and the mean divergence of the wind field during the ozone season (**Fig. 7a**) and Chicago exceedance days (**Fig. 7b**). In both composites, the average wind pattern along the Lake Michigan coastline (during the TROPOMI satellite overpass time) resembles a thermally direct circulation known as the lake breeze in which the wind blows from over the lake and onto the land (Lyons, 1972; Laird et al., 2001). The mean wind field divergence values occur in two regimes: (1) positive values indicating divergence, which strongly occurs over the lake, and (2) negative values indicating convergence, which occurs most strongly along the western Lake Michigan coastline during the study period. In the difference plot (**Fig. 7c**), mean divergence values are more negative along the western Lake Michigan coastline and are more positive over the southern part of the lake during exceedance days. This indicates that the lake breeze circulation is stronger during Chicago exceedance days relative to all days across the O_3 season. Because the lake breeze is a thermally direct circulation, the strengthening during Chicago exceedance days suggests that land temperatures are warmer during exceedance days. This result is consistent with the finding that mean HCHO levels are greater during exceedance days. Additionally, these findings are also in alignment with other studies that find that O_3 is often produced when both NO_x and VOCs are present in a shallow marine boundary layer above Lake Michigan; the high O_3 concentrations are then pushed onshore by the lake breeze, resulting in counties along the lakeshore having elevated O_3 levels (Dye et al., 1995; Stanier et al., 2021; Cleary et al., 2022; Wagner et al., 2022). Statistics for these composites can be found in **Appendix Table C1**.

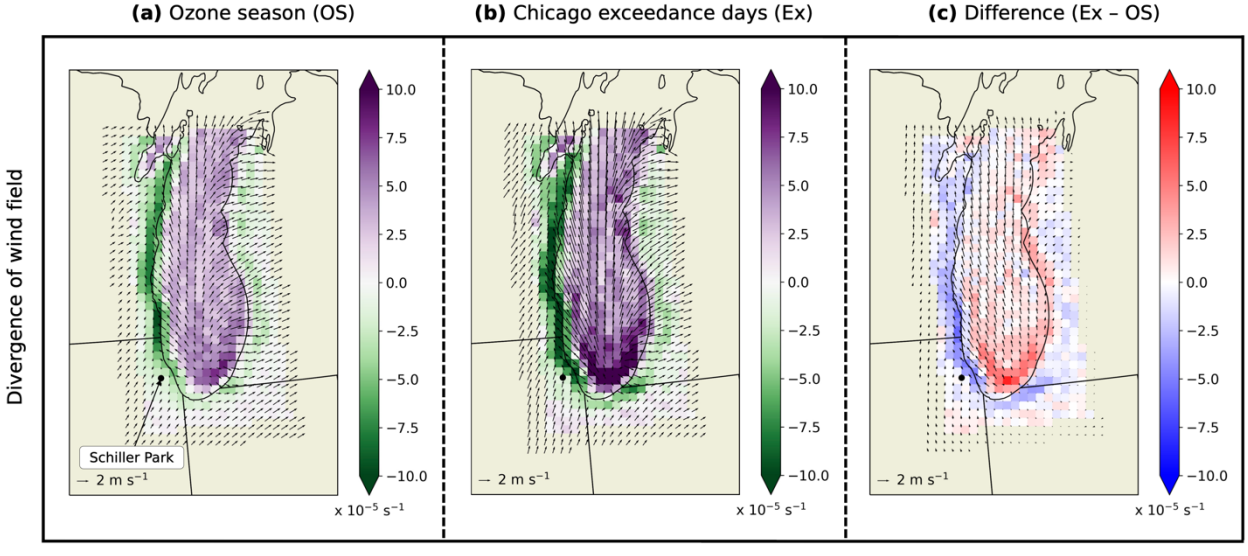

Figure 7: Divergence values of the wind field (calculated from 2019–2021 mean wind vectors) in the Lake Michigan region during: (a) the ozone season (OS), (b) Chicago ozone exceedance days (Ex), and (c) the difference between them (Ex – OS). Mean 10-meter winds are represented by arrows. In (a) and (b), positive (purple) values indicate divergence while negative (green) values indicate convergence.

https://doi.org/10.5194/egusphere-2022-1154
Preprint. Discussion started: 9 December 2022

Figure 8 shows histogram plots of the TROPOMI composite values of mean NO_2, HCHO, FNR, and wind divergence values during the ozone season and Chicago exceedance days. Two-sample Kolmogorov-Smirnov tests indicate that the differences between the ozone season and Chicago exceedance day distributions are statistically significant for all four parameters at the 99 % confidence level. These tests and histogram comparison plots provide more detail to the previous analyses. NO_2 values (**Fig. 8a**) look similar in both composites. However, there is a notable increase in the maximum NO_2 value from 5.69 x 10^{15} to 7.60 x 10^{15} mol cm^{-2} during Chicago exceedance days. The comparison of HCHO values (**Fig. 8b**) shows a large shift in HCHO levels to higher values during Chicago exceedance days. Statistically higher FNR values on Chicago exceedance days (**Fig. 8c**) are driven by higher regional HCHO concentrations (as opposed to changes in NO_2 levels). Finally, the widening of the wind divergence distribution to more negative values and greater positive values (**Fig. 8d**) further demonstrates the strengthening of the lake breeze circulation during exceedance days.

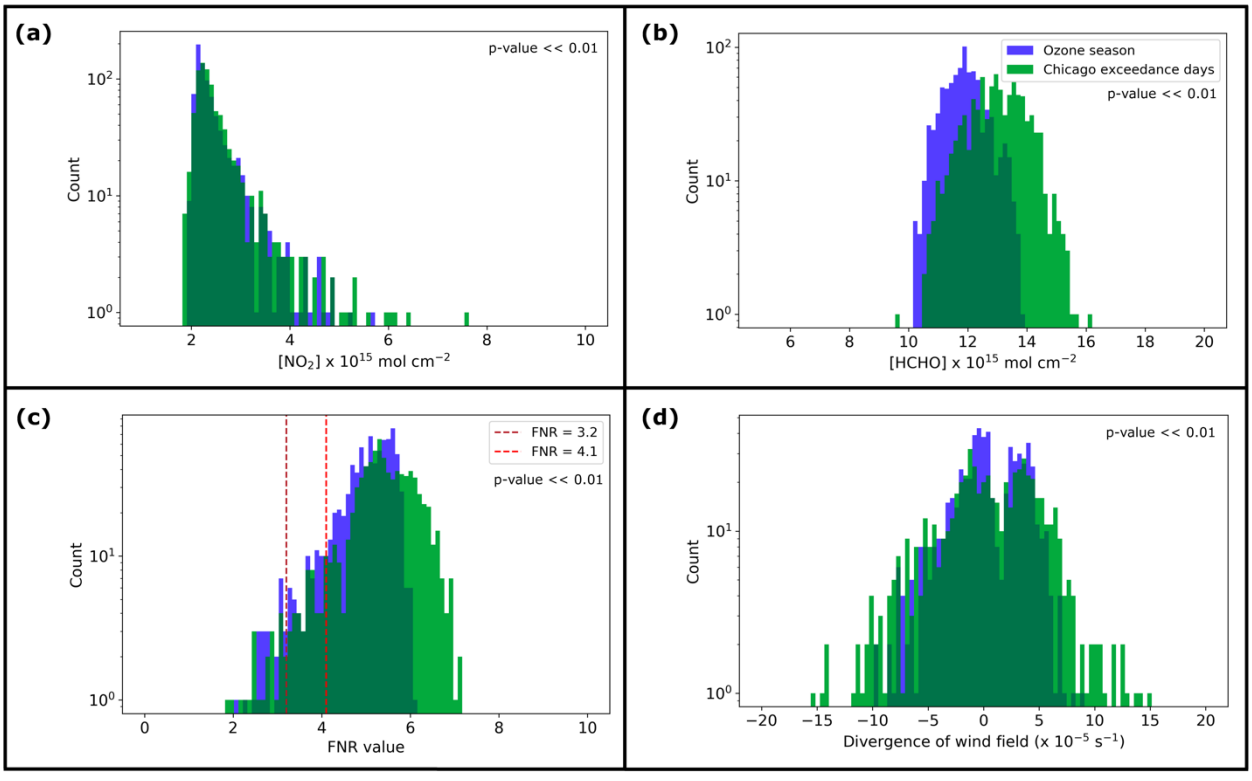

Figure 8: Histogram plots comparing the distributions of (blue) ozone season values and (green) Chicago ozone exceedance day values (from Figures 3, 4, 5, and 7) of: (a) NO_2, (b) HCHO, (c) FNRs, and (d) wind field divergence.

https://doi.org/10.5194/egusphere-2022-1154
Preprint. Discussion started: 9 December 2022

3.3 Comparison of weekday and weekend TROPOMI composites

Figure 9 displays composite mean NO_2 levels derived from TROPOMI data during weekdays (**Fig. 9a**) and weekends (**Fig. 9b**), along with mean 10-meter wind vectors. During weekdays, mean NO_2 levels range from 1.91 x 10^{15} to 6.45 x 10^{15} mol cm^{-2}, with a regional average of 2.49 x 10^{15} mol cm^{-2}. During weekends, mean NO_2 levels range from 1.82 x 10^{15} to 4.11 x 10^{15} mol cm^{-2}, with a regional average of 2.31 x 10^{15} mol cm^{-2}. Additional statistics for these composites can be found in **Appendix Table C2**. **Figure 9c**, the difference between the weekend and weekday composites, shows significantly lower mean NO_2 levels in the Chicago metropolitan area on weekends. The regional average change is a decrease of 0.18 x 10^{15} mol cm^{-2} on weekends, with the greatest decrease of 2.60 x 10^{15} mol cm^{-2} occurring in the urban core of Chicago. This result is expected as NO_x emissions generally decrease due to less road traffic volume on weekends, especially from heavy-duty diesel trucks (Demetillo et al., 2021).

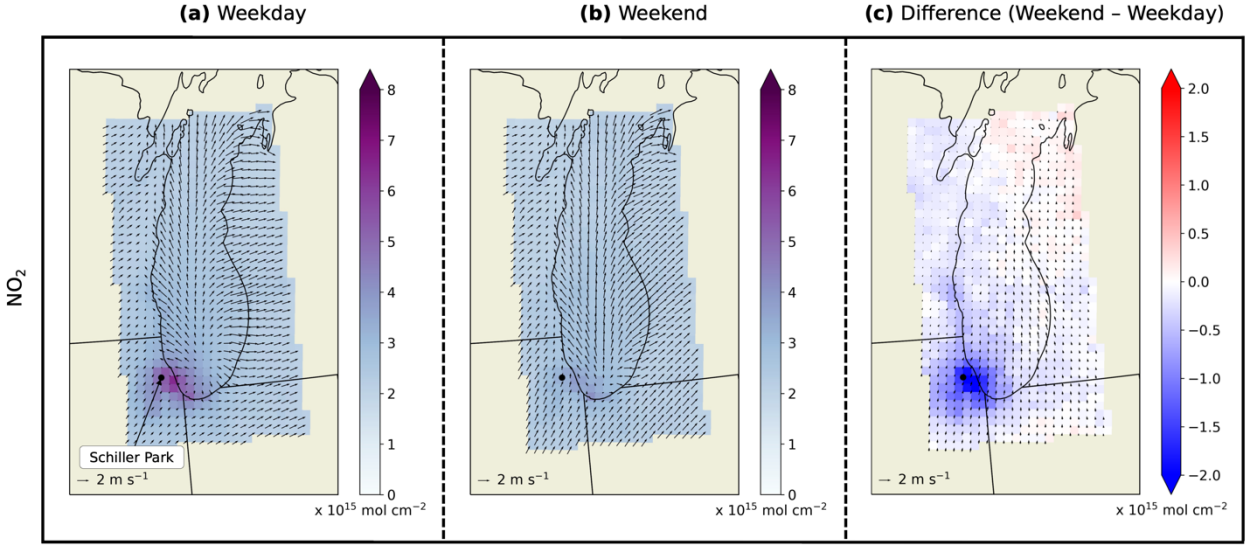

Figure 9: TROPOMI-derived composites of 2019–2021 mean tropospheric NO_2 in the Lake Michigan region during: (a) weekdays, (b) weekends, and (c) the difference between them (weekend – weekday). Mean 10-meter winds are represented by arrows.

https://doi.org/10.5194/egusphere-2022-1154
Preprint. Discussion started: 9 December 2022

Figure 10 displays composite mean HCHO levels derived from TROPOMI data during weekdays (**Fig. 10a**) and weekends (**Fig. 10b**), along with mean 10-meter wind vectors. During weekdays, mean HCHO levels range from 10.0 x 10^{15} to 13.9 x 10^{15} mol cm^{-2}, with a regional average of 11.8 x 10^{15} mol cm^{-2}. During weekends, mean HCHO levels range from 9.74 x 10^{15} to 14.3 x 10^{15} mol cm^{-2}, with a regional average of 12.0 x 10^{15} mol cm^{-2}. Additional statistics for these composites can be found in **Appendix Table C2**. **Figure 10c**, the difference between the weekend and weekday composites, shows that changes in HCHO levels are mixed as some areas have higher HCHO concentrations on weekends while others have lower concentrations. The average difference is a small increase of 0.21 x 10^{15} mol cm^{-2} on weekends. This slight increase could be due to NO_x emissions differences between weekdays and weekends. For example, the principal sink of NO_x is oxidation by hydroxyl radicals (·OH) to nitric acid (HNO_3); therefore, lower NO_x levels could lead to increased ·OH concentrations and thus increased production of secondary HCHO (Jacob, 1999). Further research is needed to investigate this hypothesis.

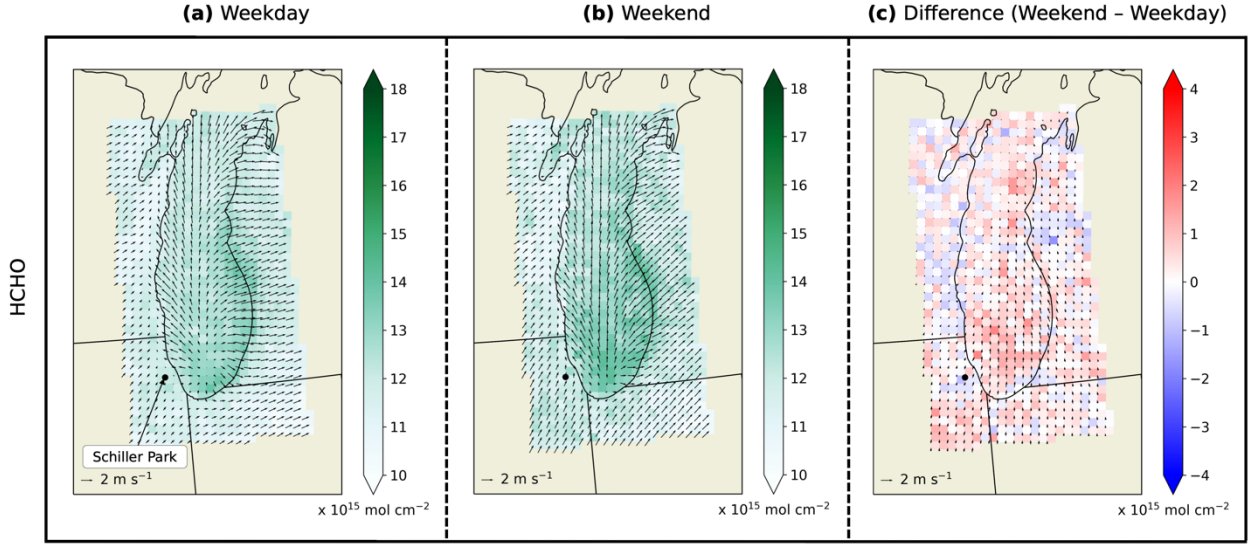

Figure 10: TROPOMI-derived composites of 2019–2021 mean tropospheric HCHO in the Lake Michigan region during: (a) weekdays, (b) weekends, and (c) the difference between them (weekend – weekday). Mean 10-meter winds are represented by arrows.

https://doi.org/10.5194/egusphere-2022-1154
Preprint. Discussion started: 9 December 2022

Figure 11 displays composite mean FNR values during weekdays (**Fig. 11a**) and weekends (**Fig. 11b**), along with mean 10-meter winds. During weekdays, mean FNR values range from 1.88 to 6.23, with a regional average of 4.90. During weekends, mean FNR values range from 2.94 to 6.53, with a regional average of 5.26. Additional statistics for these composites can be found in **Appendix Table C2**. **Figure 11c**, the difference between the weekend and weekday composites, shows that mean FNR values increase for much of the domain on weekends, with the greatest increases in the Chicago metropolitan area, indicating greater O_3 chemistry sensitivity to NO_x.

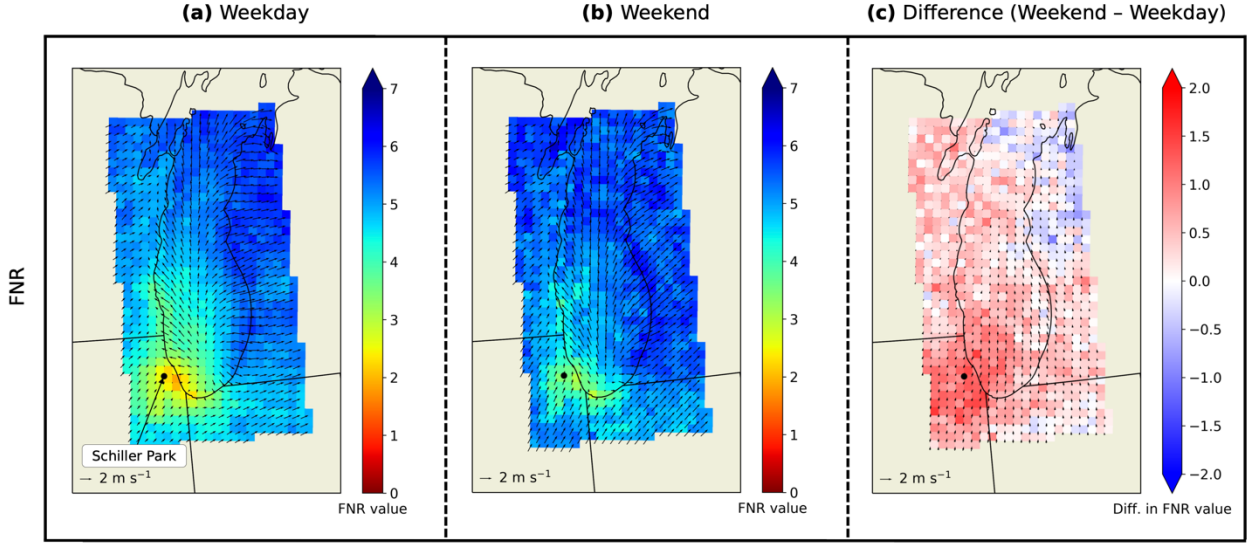

Figure 11: TROPOMI-derived 2019–2021 FNR values in the Lake Michigan region during: (a) weekdays, (b) weekends, and (c) the difference between them (weekend – weekday). Mean 10-meter winds are represented by arrows.

https://doi.org/10.5194/egusphere-2022-1154
Preprint. Discussion started: 9 December 2022

When the FNR values are interpreted using the J20 thresholds, we see notable geographical differences in O_3 chemistry sensitivity between weekdays (**Fig. 12a**) and weekends (**Fig. 12b**). The area classified as VOC-sensitive decreases from 4.3 % on weekdays to 0.2 % on weekends; only the urban core of Chicago, Illinois, and industrial areas near Gary, Indiana, remain VOC-sensitive. The transition zone also decreases from 9.1 % to 3.4 % of the area on weekends, with only grid boxes containing the CMA, Milwaukee (Wisconsin), and Gary (Indiana) indicating transitional chemistry. The area classified as NO_x-sensitive increases by about 10 % on weekends, largely due to the areas surrounding the Chicago metropolitan area and the Lake Michigan coastline between Illinois and Wisconsin changing from VOC-sensitive or transitional to becoming NO_x-sensitive.

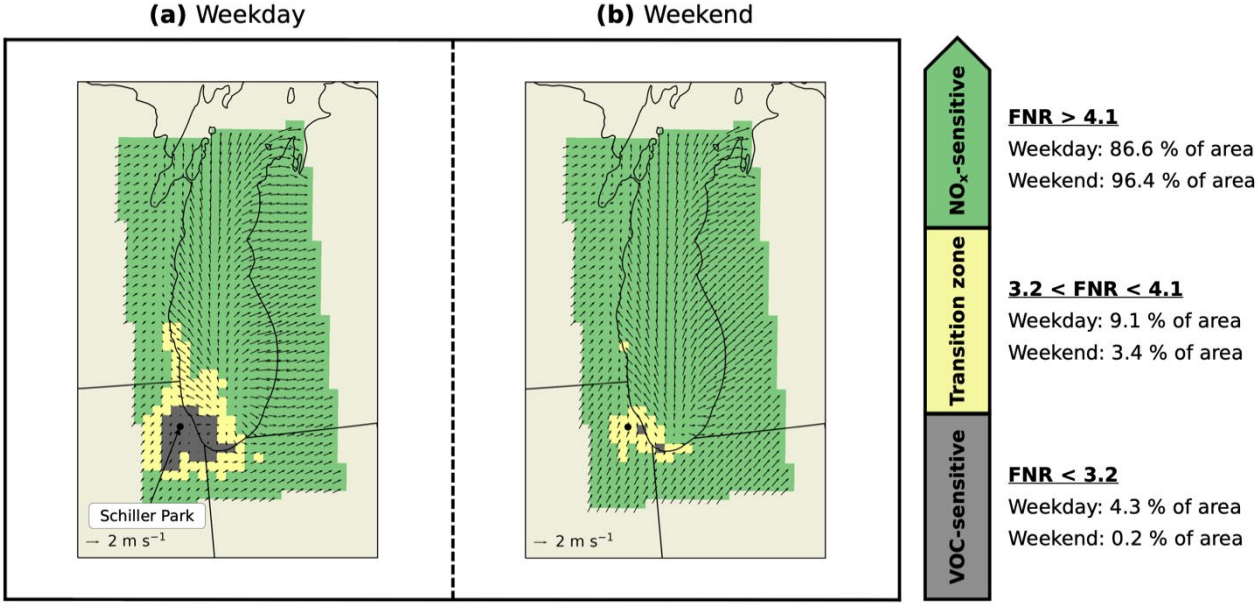

Figure 12: J20 threshold interpretation of 2019–2021 ozone–NO_x–VOC sensitivity in the Lake Michigan region during: (a) weekdays and (b) weekends. Mean 10-meter winds are represented by arrows.

https://doi.org/10.5194/egusphere-2022-1154
Preprint. Discussion started: 9 December 2022

Figure 13 displays plots of mean 10-meter wind vectors and the mean divergence of the wind field during weekdays (**Fig. 13a**) and weekends (**Fig. 13b**). Similar to the ozone season and Chicago ozone exceedance day composites, the weekday and weekend composites indicate that the average wind pattern along the Lake Michigan coastline (during the TROPOMI satellite overpass time) resembles a lake breeze circulation. The difference between the composites (**Fig. 13c**) reveals relatively small differences between weekends and weekdays in the mean divergence of the wind field (compared to the difference between the ozone season and Chicago exceedance day composites). Additionally, the average wind speed and direction is approximately the same between weekdays and weekends, as expected. Statistics for these composites can be found in **Appendix Table C2**.

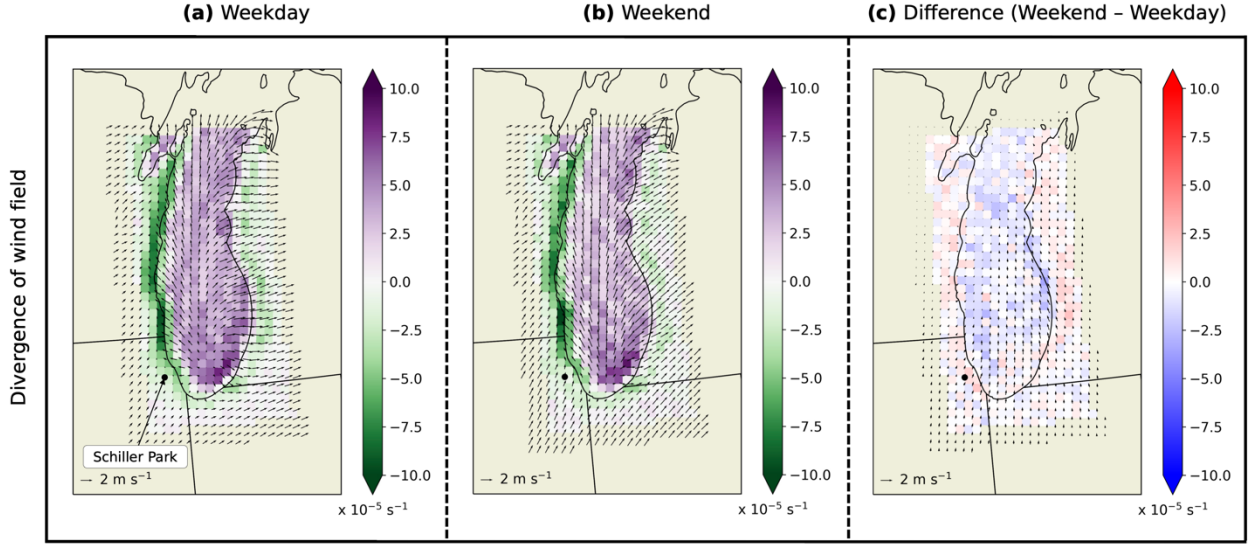

Figure 13: Divergence values of the wind field (calculated from 2019–2021 mean 10-meter wind vectors) in the Lake Michigan region during: (a) weekdays, (b) weekends, and (c) the difference between them (weekend – weekday). Mean 10-meter winds are represented by arrows. In (a) and (b), positive (purple) values indicate divergence while negative (green) values indicate convergence.

https://doi.org/10.5194/egusphere-2022-1154
Preprint. Discussion started: 9 December 2022

Figure 14 shows histogram plots of the TROPOMI composites values during weekdays (blue) and weekends (green). Two-sample Kolmogorov-Smirnov tests indicate that the differences between the weekday and weekend distributions are statistically significant for mean NO_2, HCHO, and FNR values at the 99 % confidence level, while the distributional differences for mean wind divergence values are not statistically significant at the 99 % confidence level. NO_2 levels are shifted to lower values on weekends; in particular, the weekend histogram lacks the tail of higher NO_2 values as compared to the weekday histogram (**Fig. 14a**). The comparison of HCHO values shows a slight shift to higher HCHO levels during weekends (**Fig. 14b**). On weekends, FNR values are shifted to the right (**Fig. 14c**) due to both slightly higher HCHO and lower NO_2 values. The smaller low tail of the FNR weekend histogram is driven by shifts to higher FNR values in the Chicago metropolitan area and its surroundings primarily due lower NO_2 levels. Finally, there does not appear to be a consistent pattern in the differences between wind divergence on weekdays and weekends (**Fig. 14d**).

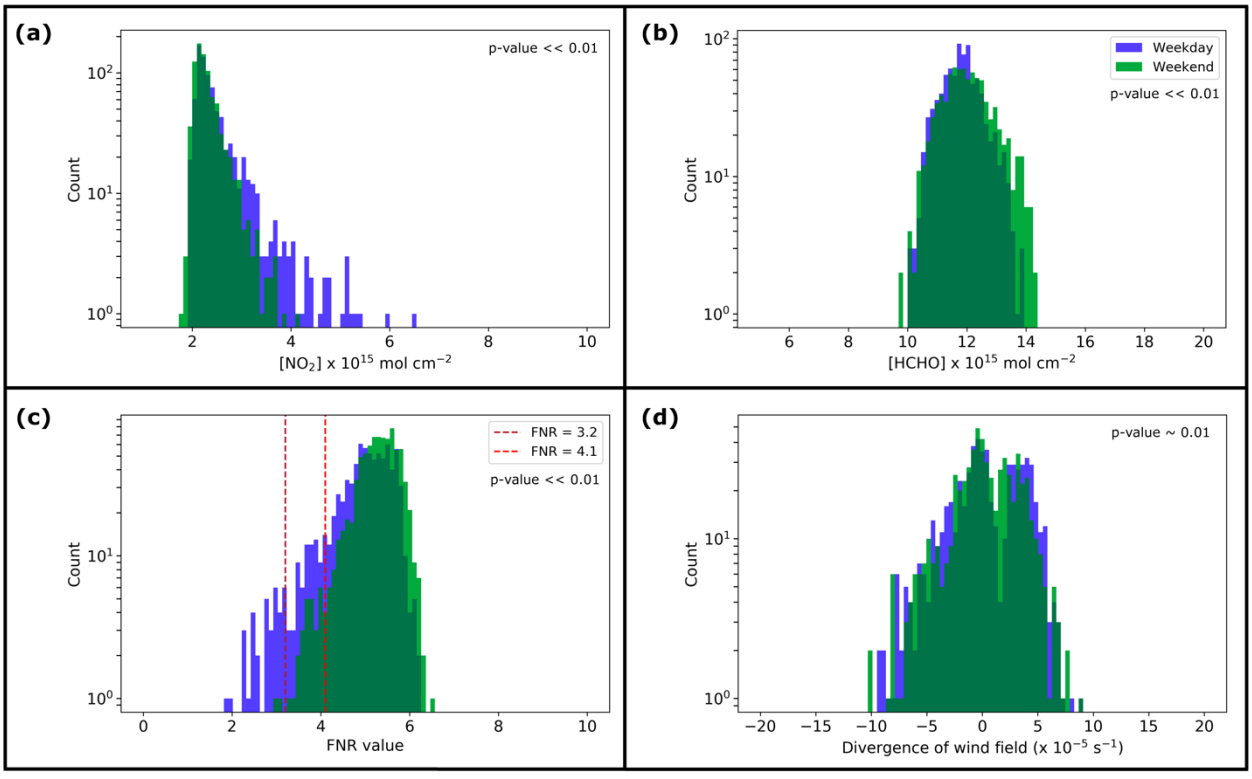

Figure 14: Histogram plots comparing the distributions of (blue) weekday values and (green) weekend values (from Figures 9, 10, 11, and 13) of: (a) NO_2, (b) HCHO, (c) FNRs, and (d) wind field divergence.

https://doi.org/10.5194/egusphere-2022-1154
Preprint. Discussion started: 9 December 2022

3.4 Limitations

The use of TROPOMI satellite retrievals of tropospheric column HCHO and NO_2 to indicate surface O_3 chemistry sensitivity has a few limitations. First, to minimize the impacts of the lower signal-to-noise ratio of TROPOMI HCHO retrievals, we temporally aggregated the data into monthly composites. Through this process we lose the ability to detect day-to-day changes in O_3 chemistry. Furthermore, S5P is a sun-synchronous polar-orbiting satellite, and TROPOMI provides measurements at about 13:30 local solar time. However, O_3 production can occur throughout the day and its sensitivity to either NO_x or VOCs can change as the atmospheric concentrations of these gases change. Higher temporal and spatial resolution satellite measurements are needed to analyse the hourly fluctuations in O_3 chemistry sensitivity from space-based instruments.

Analysis of the ground data also reveals some limitations of using PAMS data. The current 24-hour long sampling procedure smooths out hourly fluctuations in HCHO levels that can occur throughout the day, which could lead to incorrect determinations of O_3 chemistry sensitivity when interpreting surface FNR values. Additionally, FNR threshold values can vary from airshed to airshed due to different emissions, meteorological conditions, and other environmental factors (Lu and Chang, 1998). Higher temporal resolution HCHO surface measurements are needed at more PAMS sites to better determine O_3 chemistry sensitivity FNR thresholds and how they vary both diurnally and spatially. Moreover, there is a spatial disconnect when comparing TROPOMI and PAMS FNRs: the satellite FNR values (i.e., the satellite pixels composited into a grid box) cover a larger area than the point PAMS monitor measurements. Finally, TROPOMI data represent tropospheric column densities while PAMS data represent ground-level measurements, underscoring the need to apply different O_3 chemistry threshold values to FNRs calculated from each source dataset.

4 Summary and conclusions

We assessed the ozone–NO_x–VOC sensitivity of the Lake Michigan region using formaldehyde to nitrogen dioxide concentration ratios ([HCHO]/[NO_2]; "FNRs") calculated from 2019–2021 S5P TROPOMI satellite data and 2019 PAMS surface measurements. Results from the first part of this work showed that at PAMS Site 3103 in Schiller Park, Illinois, satellite-based FNRs were always greater in value than ground-based FNRs. This highlights the need to apply different threshold values to ground (surface) and satellite (column) FNR values when determining O_3 chemistry sensitivity. Specifically, we suggest applying the Jin et al. (2020; "J20") thresholds to the satellite FNRs and the Blanchard (2020) thresholds to the PAMS FNRs presented in this work.

TROPOMI FNR composites interpreted using the J20 thresholds suggest that despite increases in regional HCHO levels during Chicago O_3 exceedance days, the Chicago metropolitan area remains VOC-sensitive due to higher NO_2 levels (note that the

https://doi.org/10.5194/egusphere-2022-1154
Preprint. Discussion started: 9 December 2022

urban core of Chicago increases in VOC sensitivity as indicated by lower FNR values on Chicago exceedance days). Although areas surrounding the Chicago metropolitan area and north along the Lake Michigan coastline to Milwaukee, Wisconsin, largely remain in the transition zone, the extent of the transition zone drops by 25% during exceedance days. The rest of the domain is still NO_x-sensitive during Chicago ozone exceedance days, but even more so (as indicated by higher FNR values) due to increased HCHO levels. Higher HCHO concentrations are likely attributed to increased temperatures during exceedance events, which leads to increased biogenic VOC emissions and increased O_3 production (Sillman and Samson, 1995). These results suggest that both VOC and NO_x emissions controls would be necessary to decrease O_3 production in the Chicago nonattainment area and for the region as a whole. Analysis of wind data shows that the typical lake breeze pattern that occurs during the TROPOMI overpass time is stronger during Chicago exceedance days, which is also likely attributable to higher land temperatures impacting this type of thermally direct circulation.

When comparing weekday and weekend TROPOMI FNR composites, there is a clear difference in O_3 chemistry sensitivity in the Chicago metropolitan area. The percent of area classified as VOC-sensitive drops from 4.3 % on weekdays to 0.2 % on weekends, driven by statistically lower weekend NO_x levels in the region. Similarly, the percent of area classified as having transitional O_3 chemistry also drops from 9.1 % on weekdays to 3.4 % on weekends due to lower NO_x levels. Although the spatial distribution of differences between weekday and weekend HCHO levels are mixed between positive and negative values, the domain average has slightly higher HCHO levels on weekends. Further research is needed to investigate the possible causes for this finding (e.g., changes in NO_x–VOC chemistry due to lower NO_x levels on weekends). Analysis also shows no major differences between wind speed, direction, and divergence between weekdays and weekends during the TROPOMI overpass time, as expected.

The TROPOMI-based FNRs analyses in this study provide a "snapshot" of the average ozone–NO_x–VOC sensitivity of the Lake Michigan region during the Sentinel-5P satellite overpass time. Although such snapshots are informative for air quality management agencies that develop O_3 attainment strategies, they miss the hourly fluctuations in atmospheric HCHO and NO_2 levels (and thus fluctuations in O_3 chemistry sensitivity) that occur throughout the day. The NASA Tropospheric Emissions: Monitoring of Pollution (TEMPO) mission will address such limitations by launching an instrument onboard a geostationary-orbiting satellite that is capable of measuring air pollutants, including HCHO and NO_2, in hourly intervals over the United States (Zoogman et al., 2017). Other geostationary-orbiting satellite instruments such as the Geostationary Environment Monitoring Spectrometer (GEMS; Choi et al., 2018) and SENTINEL-4 (Gulde et al., 2017) will also make similar measurements as TEMPO for many countries in Asia and Europe, respectively. In the future, such instruments will provide researchers with new datasets to explore how information from satellite-based [HCHO]/[NO_2] ratios can be utilized to infer surface O_3 chemistry sensitivity at unprecedented spatiotemporal scales.

https://doi.org/10.5194/egusphere-2022-1154
Preprint. Discussion started: 9 December 2022

620 **Appendices**

Appendix A. Chicago ozone exceedance days

Table A1: Dates of 2019, 2020, and 2021 O_3 exceedance days in the Chicago, Illinois, metropolitan area. An O_3 exceedance day is defined as having at least one ground monitor in the U.S. EPA Air Quality System (AQS) measuring an MDA8 O_3 value greater than 70 ppb.

2019 Dates	Number of stations	2020 Dates	Number of stations	2021 Dates	Number of stations
June 5	2	June 4	4	May 22	1
June 26	1	June 5	10	June 3	14
June 28	1	June 8	3	June 4	5
June 29	4	June 16	2	June 11	5
July 3	2	June 17	15	June 17	5
July 5	1	June 18	19	June 18	8
July 8	1	June 19	16	July 20	5
July 9	11	June 27	2	July 22	6
July 13	1	July 1	4	July 23	4
July 25	2	July 2	1	July 26	2
August 2	1	July 3	14	July 27	1
August 3	2	July 6	13	July 28	4
Total: 12 days		July 7	6	August 4	3
		July 8	4	August 7	2
		July 9	5	August 10	1
		July 17	2	August 23	1
		July 25	5	August 25	6
		August 7	1	August 26	4
		August 15	4	August 27	4
		August 21	3	September 13	1
		Total: 20 days		October 1	3
				Total: 21 days	

https://doi.org/10.5194/egusphere-2022-1154
Preprint. Discussion started: 9 December 2022

Appendix B. Derivation of the uncertainty of FNR values calculated from TROPOMI retrievals

$$FNR \pm uncertainty\ in\ FNR\ value = \frac{[NO_2] \pm uncertainty\ in\ NO_2\ retrieval}{[HCHO] \pm uncertainty\ in\ HCHO\ retrieval}$$

$$Uncertainty\ in\ FNR\ value = \sqrt{(uncertainty\ in\ NO_2\ retrieval)^2 + (uncertainty\ in\ HCHO\ retrieval)^2}$$

Note: Based on equation for uncertainty propagation for division

Retrieval species	Lower limit uncertainty	Upper limit uncertainty	Source(s)
NO_2	15 %	50 %	Boersma et al., 2018; van Geffen et al., 2021
HCHO	30 %	60 %	De Smedt et al., 2021

$$Lower\ limit\ FNR\ uncertainty = \sqrt{(0.15)^2 + (0.30)^2} \approx 0.335, or\ 33.5\ \%$$

$$Upper\ limit\ FNR\ uncertainty = \sqrt{(0.50)^2 + (0.60)^2} \approx 0.781, or\ 78.1\ \%$$

https://doi.org/10.5194/egusphere-2022-1154
Preprint. Discussion started: 9 December 2022

Appendix C. TROPOMI composite statistics

Table C1: Basic statistics for the TROPOMI typical ozone season day and Chicago ozone exceedance day composites.

		Ozone season (OS)	Chicago exceedance days (Ex)	Difference (Ex – OS)
HCHO (mol cm^{-2})	**Min.**	10.2 x 10^{15}	9.64 x 10^{15}	-0.96 x 10^{15}
	Mean	11.9 x 10^{15}	13.0 x 10^{15}	1.13 x 10^{15}
	Max.	13.8 x 10^{15}	16.2 x 10^{15}	2.67 x 10^{15}
NO_2 (mol cm^{-2})	**Min.**	1.95 x 10^{15}	1.84 x 10^{15}	-0.38 x 10^{15}
	Mean	2.44 x 10^{15}	2.51 x 10^{15}	0.08 x 10^{15}
	Max.	5.69 x 10^{15}	7.60 x 10^{15}	1.91 x 10^{15}
FNR (unitless)	**Min.**	2.12	1.84	-0.53
	Mean	4.99	5.34	0.35
	Max.	6.12	7.11	1.54
Eastward wind (m s^{-1})	**Min.**	-1.50	-2.59	-1.41
	Mean	0.82	0.78	-0.04
	Max.	1.93	2.92	0.64
Northward wind (m s^{-1})	**Min.**	-0.84	-1.25	-0.42
	Mean	0.63	1.40	0.77
	Max.	1.93	3.61	1.96
Wind divergence (s^{-1})	**Min.**	-9.63 x 10^{-5}	-15.2 x 10^{-5}	-5.82 x 10^{-5}
	Mean	0.41 x 10^{-5}	0.57 x 10^{-5}	0.16 x 10^{-5}
	Max.	8.75 x 10^{-5}	15.1 x 10^{-5}	8.65 x 10^{-5}

https://doi.org/10.5194/egusphere-2022-1154
Preprint. Discussion started: 9 December 2022

Table C2: Basic statistics for the TROPOMI weekday and weekend composites.

		Weekday	Weekend	Difference (Weekend – Weekday)
HCHO (mol cm^{-2})	**Min.**	10.0 x 10^{15}	9.74 x 10^{15}	-1.68 x 10^{15}
	Mean	11.8 x 10^{15}	12.0 x 10^{15}	0.21 x 10^{15}
	Max.	13.9 x 10^{15}	14.3 x 10^{15}	1.93 x 10^{15}
NO_2 (mol cm^{-2})	**Min.**	1.91 x 10^{15}	1.82 x 10^{15}	-2.60 x 10^{15}
	Mean	2.49 x 10^{15}	2.31 x 10^{15}	-0.18 x 10^{15}
	Max.	6.45 x 10^{15}	4.11 x 10^{15}	0.37 x 10^{15}
FNR (unitless)	**Min.**	1.88	2.94	-1.00
	Mean	4.90	5.26	0.36
	Max.	6.23	6.53	1.56
Eastward wind (m s^{-1})	**Min.**	-1.62	-1.35	-0.55
	Mean	0.80	0.86	0.06
	Max.	2.85	2.38	0.56
Northward wind (m s^{-1})	**Min.**	-1.04	-0.51	-0.31
	Mean	0.50	0.94	0.43
	Max.	1.94	1.90	1.24
Wind divergence (s^{-1})	**Min.**	-9.48 x 10^{-5}	-10.3 x 10^{-5}	-3.50 x 10^{-5}
	Mean	0.47 x 10^{-5}	0.28 x 10^{-5}	-0.19 x 10^{-5}
	Max.	8.71 x 10^{-5}	9.00 x 10^{-5}	2.39 x 10^{-5}

https://doi.org/10.5194/egusphere-2022-1154
Preprint. Discussion started: 9 December 2022

Code & data availability

Python scripts used to generate composites of TROPOMI data and analyse PAMS data as well as the TROPOMI composite data files we created in netCDF format are available upon request (send correspondence to acdan@wisc.edu). TROPOMI data can be downloaded from the NASA GES DISC website (https://disc.gsfc.nasa.gov/). PAMS data can be downloaded from the U.S. EPA Air Data website (https://www.epa.gov/outdoor-air-quality-data).

Author contribution

J. J. M. Acdan's contributions include: (1) acquiring and processing TROPOMI data, (2) processing and analysing PAMS data, (3) visualizing all data, (4) developing the methodologies, (5) interpreting the results, and (6) writing, reviewing, and editing drafts of this manuscript. R. B. Pierce's contributions include: (1) participating in the conceptualization of the study, (2) developing the methodologies, (3) supervising the project, (4) interpreting the results, and (5) reviewing and editing drafts of this manuscript. A. F. Dickens's, Z. Adelman's, and T. Nergui's contributions include: (1) conceptualizing the research project, (2) acquiring PAMS data, (3) supervising the project, (4) reviewing and editing drafts of this manuscript, and (5) providing funding support. A. F. Dickens was additionally involved in the interpretation of the results.

Competing interests

The authors declare that they have no conflict of interest.

Acknowledgements

We acknowledge funding support from the Lake Michigan Air Directors Consortium (LADCO).

https://doi.org/10.5194/egusphere-2022-1154
Preprint. Discussion started: 9 December 2022

References

Acdan, J. J. M., Vermeuel, M., Bertram, T. H., and Pierce, R. B: Observation-based analyses of the sensitivity of ozone formation in the Lake Michigan region to NO_x and VOC Emissions [Final Report prepared for the Lake Michigan Air Directors Consortium], Accessed: September 21, 2022, https://www.ladco.org/wp-content/uploads/Projects/Ozone/2020_WI-DNR_OBM_Analysis/LADCO_FinalReport_2020.pdf, 2020.

Blanchard, C. L.: Observation-based analyses of the sensitivity of ozone formation in the Lake Michigan region to NO_x and VOC Emissions [Final Report prepared for the Lake Michigan Air Directors Consortium], Accessed: October 1, 2021, https://www.ladco.org/wp-content/uploads/Projects/Ozone/2020_WI-DNR_OBM_Analysis/Blanchard_Final-Report_Sep2020.pdf, 2020.

Boersma, K. F., Eskes, H. J., Richter, A., De Smedt, I., Lorente, A., Beirle, S., van Geffen, J. H. G. M., Zara, M., Peters, E., Van Roozendael, M., Wagner, T., Maasakkers, J. D., van der A, R. J., Nightingale, J., De Rudder, A., Irie, H., Pinardi, G., Lambert, J.-C., and Compernolle, S. C.: Improving algorithms and uncertainty estimates for satellite NO_2 retrievals: results from the quality assurance for the essential climate variables (QA4ECV) project, Atmos. Meas. Tech., 11, 6651–6678, https://doi.org/10.5194/amt-11-6651-2018, 2018.

Brown-Steiner, B., Hess, P. G., and Lin, M. Y.: On the capabilities and limitations of GCCM simulations of summertime regional air quality: a diagnostic analysis of ozone and temperature simulations in the US using CESM CAM-Chem, Atmos. Environ., 101, 134–148, https://doi.org/10.1016/j.atmosenv.2014.11.001, 2015.

Chance, K.: OMI algorithm theoretical basis document [Volume IV, OMI trace gas algorithms], Accessed: May 29, 2022, https://ozoneaq.gsfc.nasa.gov/media/docs/ATBD-OMI-04.pdf, 2002.

Chang, C. Y., Faust, E., Hou, X., Lee, P., Kim, H. C., Hedquist, B. C., and Liao, K. J.: Investigating ambient ozone formation regimes in neighboring cities of shale plays in the Northeast United States using photochemical modeling and satellite retrievals, Atmos. Environ., 142, 152–170, https://doi.org/10.1016/j.atmosenv.2016.06.058, 2016.

Choi, W. J., Moon, K.-J., Yoon, J., Cho, A., Kim, S.-k., Lee, S., Ko, D. h., Kim, J., Ahn, M. H., Kim, D.-R., Kim, S.-M., Kim, J.-Y., Nicks, D., and Kim, J. S.: Introducing the geostationary environment monitoring spectrometer, J. Appl. Remote Sens., 12(4), 044005, https://doi.org/10.1117/1.JRS.12.044005, 2018.

https://doi.org/10.5194/egusphere-2022-1154
Preprint. Discussion started: 9 December 2022

Cleary, P. A., Dickens, A., McIlquham, M., Sanchez, M., Geib K., Hedberg C., Hupy J., Watson H. W., Fuoco M., Olson E. R., Pierce R. B., Stanier, C., Long, R., Valin, L., Conley, S., and Smith, M.: Impacts of lake breeze meteorology on ozone gradient observations along Lake Michigan shorelines in Wisconsin, Atmos. Environ., 269, 118834, https://doi.org/10.1016/j.atmosenv.2021.118834, 2022.

De Smedt, I., Pinardi, G., Vigouroux, C., Compernolle, S., Bais, A., Benavent, N., Boersma, F., Chan, K.-L., Donner, S., Eichmann, K.-U., Hedelt, P., Hendrick, F., Irie, H., Kumar, V., Lambert, J.-C., Langerock, B., Lerot, C., Liu, C., Loyola, D., Piters, A., Richter, A., Rivera Cárdenas, C., Romahn, F., Ryan, R. G., Sinha, V., Theys, N., Vlietinck, J., Wagner, T., Wang, T., Yu, H., and Van Roozendael, M.: Comparative assessment of TROPOMI and OMI formaldehyde observations and validation against MAX-DOAS network column measurements, Atmos. Chem. Phys., 21, 12561–12593, https://doi.org/10.5194/acp-21-12561-2021, 2021.

De Smedt, I., Romahn, F., and Eichmann, K.-U.: S5P mission performance centre formaldehyde [L2__HCHO___] readme [V02.03.00], Accessed: May 29, 2022, https://sentinel.esa.int/documents/247904/3541451/Sentinel-5P-Formaldehyde-Readme.pdf, 2022.

De Smedt, I., Theys, N., Yu, H., Danckaert, T., Lerot, C., Compernolle, S., Van Roozendael, M., Richter, A., Hilboll, A., Peters, E., Pedergnana, M., Loyola, D., Beirle, S., Wagner, T., Eskes, H., van Geffen, J., Boersma, K. F., and Veefkind, P.: Algorithm theoretical baseline for formaldehyde retrievals from S5P TROPOMI and from the QA4ECV project, Atmos. Meas. Tech., 11, 2395–2426, https://doi.org/10.5194/amt-11-2395-2018, 2018.

Demetillo, M. A. G., Harkins, C., McDonald, B. C., Chodrow, P. S., Sun, K., and Pusede, S. E.: Space-based observational constraints on NO_2 air pollution inequality from diesel traffic in major US cities, Geophys. Res. Lett., 48(17), e2021GL094333, https://doi.org/10.1029/2021GL094333, 2021.

Duncan, B. N., Yoshida, Y., Olson, J. R., Sillman, S., Martin, R. V., Lamsal, L., Hu, Y., Pickering, K. E., Retscher, C., Allen, D. J., and Crawford, J. H.: Application of OMI observations to a space-based indicator of NO_x and VOC controls on surface ozone formation. Atmos. Environ., 44(18), 2213–2223. https://doi.org/10.1016/j.atmosenv.2010.03.010, 2010.

Dye, T. S., Roberts, P. T., and Korc, M. E.: Observations of transport processes for ozone and ozone precursors during the 1991 Lake Michigan Ozone Study, J. Appl. Meteorol. Climatol., 34(8), 1877–1889, https://doi.org/10.1175/1520-0450(1995)034%3C1877:OOTPFO%3E2.0.CO;2, 1995.

https://doi.org/10.5194/egusphere-2022-1154
Preprint. Discussion started: 9 December 2022

Eskes, H. J., and Eichmann, K.-U.: S5P mission performance centre nitrogen dioxide [L2__NO2___] readme [V02.03.01], Accessed: May 29, 2022, https://sentinel.esa.int/documents/247904/3541451/Sentinel-5P-Nitrogen-Dioxide-Level-2-Product-Readme-File, 2021.

Eskes, H. J., van Geffen, J., Boersma, F., Eichmann, K.-U., Apituley, A., Pedergnana, M., Sneep, M., Veefkind, J. P., and Loyola, D.: Sentinel-5 precursor/TROPOMI level 2 product user manual nitrogendioxide [issue 4.0.2], Accessed: May 29, 2022, https://sentinel.esa.int/documents/247904/2474726/Sentinel-5P-Level-2-Product-User-Manual-Nitrogen-Dioxide, 2021.

German Aerospace Center (DLR): Sentinel-5P TROPOMI Tropospheric Formaldehyde HCHO 1-Orbit L2 7km x 3.5km (Copernicus Sentinel data processed by ESA), Greenbelt, MD, USA, Goddard Earth Sciences Data and Information Services Center (GES DISC), Accessed: October 11, 2021, https://doi.org/10.5270/S5P-tjlxfd2, 2019.

German Aerospace Center (DLR): Sentinel-5P TROPOMI Tropospheric Formaldehyde HCHO 1-Orbit L2 5.5km x 3.5km (Copernicus Sentinel data processed by ESA), Greenbelt, MD, USA, Goddard Earth Sciences Data and Information Services Center (GES DISC), Accessed: October 11, 2021, https://doi.org/10.5270/S5P-vg1i7t0, 2020.

Gulde, S. T., Kolm, M. G., Smith, D. J., Maurer, R., Bazalgette Courrèges-Lacoste, G., Sallusti, M., and Bagnasco, G.: Sentinel 4: a geostationary imaging UVN spectrometer for air quality monitoring: status of design, performance and development, International Conference on Space Optics — ICSO 2014, Proceedings Volume 10563, 1056341, https://doi.org/10.1117/12.2304099, 2017.

Haagen-Smit, A. J.: Chemistry and physiology of Los Angeles smog, Ind. Eng. Chem., 44(6), 1342–1346. https://doi.org/10.1021/ie50510a045, 1952.

Jacob, D. J.: Introduction to atmospheric chemistry, Princeton University Press, https://doi.org/10.1515/9781400841547, 1999.

Jacob, D. J.: Heterogeneous chemistry and tropospheric ozone, Atmos. Environ., 34(12–14), 2131–2159. https://doi.org/10.1016/S1352-2310(99)00462-8, 2000.

Jerrett, M., Burnett, R. T., Pope III, C. A., Ito, K., Thurston, G., Krewski, D., Shi, Y., Calle, E., and Thun, M: Long-term ozone exposure and mortality, N. Engl. J. Med., 360(11), 1085–1095. https://doi.org/10.1056/NEJMoa0803894, 2009.

https://doi.org/10.5194/egusphere-2022-1154
Preprint. Discussion started: 9 December 2022

Jin, X., Fiore, A. M., Boersma, K. F., De Smedt, I., and Valin, L.: Inferring changes in summertime surface ozone–NO_x–VOC chemistry over U.S. urban areas from two decades of satellite and ground-based observations, Environ. Sci. Tech., 54(11), 6518–6529, https://doi.org/10.1021/acs.est.9b07785, 2020.

Jin, X., Fiore, A. M., Murray, L. T., Valin, L. C., Lamsal, L. N., Duncan, B., Boersma, K. F., De Smedt, I., Gonzalez Abad, G., Chance, K., and Tonnesen, G. S.: Evaluating a space-based indicator of surface ozone-NO_x-VOC sensitivity over midlatitude source regions and application to decadal trends. Journal of Geophysical Research: Atmospheres, 122(19), 10439–10461. https://doi.org/10.1002/2017JD026720, 2017.

Jin, X., and Holloway, T.: Spatial and temporal variability of ozone sensitivity over China observed from the Ozone Monitoring Instrument, J. Geophys. Res. Atmos., 120(14), 7229–7246. https://doi.org/10.1002/2015JD023250, 2015.

Kalnay-Rivas, and Hoitsma, D.: Documentation of the fourth order band model [NASA Technical Memorandum 80608], Accessed: June 6, 2022, https://ntrs.nasa.gov/api/citations/19800009376/downloads/19800009376.pdf, 1979.

Koninklijk Nederlands Meteorologisch Instituut (KNMI): Sentinel-5P TROPOMI Tropospheric NO2 1-Orbit L2 7km x 3.5km (Copernicus Sentinel data processed by ESA), Greenbelt, MD, USA, Goddard Earth Sciences Data and Information Services Center (GES DISC), Accessed: October 11, 2021, https://doi.org/10.5270/S5P-s4ljg54, 2018.

Koninklijk Nederlands Meteorologisch Instituut (KNMI): Sentinel-5P TROPOMI Tropospheric NO2 1-Orbit L2 5.5km x 3.5km (Copernicus Sentinel data processed by ESA), Greenbelt, MD, USA, Goddard Earth Sciences Data and Information Services Center (GES DISC), Accessed: October 11, 2021, https://doi.org/10.5270/S5P-s4ljg54, 2019.

Koninklijk Nederlands Meteorologisch Instituut (KNMI): Sentinel-5P TROPOMI Tropospheric NO2 1-Orbit L2 5.5km x 3.5km (Copernicus Sentinel data processed by ESA), Greenbelt, MD, USA, Goddard Earth Sciences Data and Information Services Center (GES DISC), Accessed: October 11, 2021, https://doi.org/10.5270/S5P-9bnp8q8, 2021.

Laird, N. F., Kristovich, D. A. R., Liang, X.-Z., Arritt, R. W., and Labas, K.: Lake Michigan Lake breezes: climatology, local forcing, and synoptic environment, J. Appl. Meteorol. Climatol., 40(3), 409–424, https://doi.org/10.1175/1520-0450(2001)040%3C0409:LMLBCL%3E2.0.CO;2, 2001.

Lu, C. H., and Chang, J. S.: On the indicator-based approach to assess ozone sensitivities and emissions features, J. Geophys. Res., 103(D3): 3453–3462, https://doi.org/10.1029/97JD03128, 1998.

https://doi.org/10.5194/egusphere-2022-1154
Preprint. Discussion started: 9 December 2022

Ludewig, A., Kleipool, Q., Bartstra, R., Landzaat, R., Leloux, J., Loots, E., Meijering, P., van der Plas, E., Rozemeijer, N., Vonk, F., and Veefkind, P.: In-flight calibration results of the TROPOMI payload on board the Sentinel-5 Precursor satellite, Atmos. Meas. Tech., 13, 3561–3580, https://doi.org/10.5194/amt-13-3561-2020, 2020.

Lyons, W. A.: The climatology and prediction of the Chicago lake breeze, J. Appl. Meteorol. Climatol., 11(8), 1259–1270, https://doi.org/10.1175/1520-0450(1972)011%3C1259:TCAPOT%3E2.0.CO;2, 1972.

Martin, R. V., Fiore, A. M., and Van Donkelaar, A.: Space-based diagnosis of surface ozone sensitivity to anthropogenic emissions, Geophys. Res. Lett., 31(6), L06120, https://doi.org/10.1029/2004GL019416, 2004.

Milford, J. B., Russell, A. G., and McRae, G. J.: A new approach to photochemical pollution control: implications of spatial patterns in pollutant responses to reductions in nitrogen oxides and reactive organic gas emissions, Environ. Sci. Technol., 23(10), 1290–1301, https://doi.org/10.1021/es00068a017, 1989.

Nuvolone, D., Petri, D., and Voller, F.: The effects of ozone on human health, Environ. Sci. Pollut. Res., 25, 8074–8088, https://doi.org/10.1007/s11356-017-9239-3, 2018.

Ruiz-Suárez, J. C., Ruiz-Suárez, L. G., Gay, C., Castro, T., Montero, M., Eidels-Dubovoi, S., and Muhlia, A.: Photolytic rates for NO_2, O_3 and HCHO in the atmosphere of Mexico City, Atmos. Environ. Part A. General Topics, 27(3), 427–430, https://doi.org/10.1016/0960-1686(93)90116-G, 1993.

Schroeder, J. R., Crawford, J. H., Fried, A., Walega, J., Weinheimer, A., Wisthaler, A., Muller, M., Mikoviny, T., Chen, G., Shook, M., Blake, D. R., and Tonnesen, G. S.: New insights into the column CH_2O/NO_2 ratio as an indicator of near-surface ozone sensitivity, J. Geophys. Res. Atmos., 122(16), 8885–8907, https://doi.org/10.1002/2017JD026781, 2017.

Sillman, S.: The use of NO_y, H_2O_2, and HNO_3 as indicators for ozone-NO_x-hydrocarbon sensitivity in urban locations. J. Geophys. Res. Atmos., 100(D7), 14175–14188, http://dx.doi.org/10.1029/94JD02953, 1995.

Sillman, S., and Samson, P. J.: Impact of temperature on oxidant photochemistry in urban, polluted rural and remote environments, J. Geophys. Res. Atmos., 100(D6), 11497–11508, https://doi.org/10.1029/94JD02146, 1995.

Stanier, C. O., Pierce, R. B., Abdi-Oskouei, M., Adelman, Z. E., Al-Saadi, J., Alwe, H. D., Bertram, T. H., Carmichael, G. R., Christiansen, M. B., Cleary, P. A., Czarnetzki, A. C., Dickens, A. F., Fuoco, M. A., Hughes, D. D., Hupy, J. P., Janz, S. J., Judd, L. M., Kenski, D., Kowalewski, M. G., Long, R. W., Millet, D. B., Novak, G., Roozitalab, B., Shaw, S. L., Stone, E. A.,

https://doi.org/10.5194/egusphere-2022-1154
Preprint. Discussion started: 9 December 2022

Szykman, J., Valin, L., Vermeuel, M., Wagner, T. J., Whitehill, A. R., and Williams, D. J.: Overview of the Lake Michigan Ozone Study 2017, Bull. Amer. Meteor., 102(12), E2207–E2225, https://journals.ametsoc.org/view/journals/bams/102/12/BAMS-D-20-0061.1.xml, 2021.

Thornton, J. A., Wooldridge, P. J., Cohen, R. C., Martinez, M., Harder, H., Brune, W. H., Williams, E. J., Roberts, J. M., Fehsenfeld, F. C., Hall, S. R., Shetter, R. E., Wert, B. P., and Fried, A.: Ozone production rates as a function of NO_x abundances and HO_x production rates in the Nashville urban plume, J. Geophys. Res., 107(D12), 4146, https://doi.org/10.1029/2001JD000932, 2002.

Tonnesen, G. S., and Dennis, R. L.: Analysis of radical propagation efficiency to assess ozone sensitivity to hydrocarbons and NO_x 2. Long-lived species as indicators of ozone concentration sensitivity. J. Geophys. Res., 105(D7), 9227–9241. https://doi.org/10.1029/1999JD900372, 2000.

Turner, M. C., Jerrett, M., Pope II, C. A., Krewski, D., Gapstur, S. M., Diver, W. R., Beckerman, B. S., Marshall, J. D., Su, J., Crouse, D. L., and Burnett, R. T.: Long-term ozone exposure and mortality in a large prospective study, Am. J. Respir. Crit. Care Med., 193(10), 1134–1142. https://doi.org/10.1164/rccm.201508-1633OC, 2016.

United States Environmental Protection Agency (U.S. EPA): 2017 National Emissions Inventory (NEI) data, Accessed: June 29, 2022, https://www.epa.gov/air-emissions-inventories/2017-national-emissions-inventory-nei-data, 2021.

United States Environmental Protection Agency (U.S. EPA): NAAQS table, Accessed: June 27, 2022, https://www.epa.gov/criteria-air-pollutants/naaqs-table, 2022a.

United States Environmental Protection Agency (U.S. EPA): 8-hour ozone nonattainment areas (2015 standard), Accessed: June 27, 2022, https://www3.epa.gov/airquality/greenbook/map8hr_2015.html, 2022b.

Valin, L. C., Fiore, A. M., Chance, K., and González Abad, G.: The role of OH production in interpreting the variability of CH_2O columns in the southeast U.S., J. Geophy. Res. Atmos., 121(1), 478–493. https://doi.org/10.1002/2015JD024012, 2016.

van Geffen, J., Boersma, K. F., Eskes, H., Sneep, M., ter Linden, M., Zara, M., and Veefkind, J. P.: S5P TROPOMI NO_2 slant column retrieval: method, stability, uncertainties and comparisons with OMI, Atmos. Meas. Tech., 13, 1315–1335, https://doi.org/10.5194/amt-13-1315-2020, 2020.

https://doi.org/10.5194/egusphere-2022-1154
Preprint. Discussion started: 9 December 2022

van Geffen, J. Eskes, H. J., Boersma, K. F., and Veefkind, J. P.: TROPOMI ATBD of the total and tropospheric NO_2 data products, Royal Netherlands Meteorological Institute, Accessed: May 29, 2022, https://sentinel.esa.int/documents/247904/2476257/Sentinel-5P-TROPOMI-ATBD-NO2-data-products, 2021.

van Geffen, J., Eskes, H., Compernolle, S., Pinardi, G., Verhoelst, T., Lambert, J.-C., Sneep, M., ter Linden, M., Ludewig, A., Boersma, K. F., and Veefkind, J. P.: Sentinel-5P TROPOMI NO_2 retrieval: impact of version v2.2 improvements and comparisons with OMI and ground-based data, Atmos. Meas. Tech., 15, 2037–2060, https://doi.org/10.5194/amt-15-2037-2022, 2022.

Veefkind, J. P., Aben, I., McMullan, K., Förster, H., de Vries, J., Otter, G., Claas, J., Eskes, H. J., de Haan, J. F., Kleipool, Q., van Weele, M., Hasekamp, O., Hoogeveen, R., Landgraf, J., Snel, R., Tol, P., Ingmann, P., Voors, R., Kruizinga, B., Vink, R., Visser, H., and Levelt, P. F.: TROPOMI on the ESA Sentinel-5 Precursor: A GMES mission for global observations of the atmospheric composition for climate, air quality and ozone layer applications, Remote Sens. Environ., 120, 70–83. https://doi.org/10.1016/j.rse.2011.09.027, 2012.

Vermeuel, M. P., Novak, G. A., Alwe, H. D., Hughes, D. D., Kaleel, R., Dickens, A. F., Kenski, D., Czarnetzki, A. C., Stone, E. A., Stanier, C. O., Pierce, R. B., Millet, D. B., and Bertram, T. H.: Sensitivity of ozone production to NO_x and VOC along the Lake Michigan coastline, J. Geophys. Res. Atmos., 124(20), 10989–11006. https://doi.org/10.1029/2019JD030842, 2019.

Vigouroux, C., Langerock, B., Bauer Aquino, C. A., Blumenstock, T., Cheng, Z., De Mazière, M., De Smedt, I., Grutter, M., Hannigan, J. W., Jones, N., Kivi, R., Loyola, D., Lutsch, E., Mahieu, E., Makarova, M., Metzger, J.-M., Morino, I., Murata, I., Nagahama, T., Notholt, J., Ortega, I., Palm, M., Pinardi, G., Röhling, A., Smale, D., Stremme, W., Strong, K., Sussmann, R., Té, Y., van Roozendael, M., Wang, P., and Winkler, H.: TROPOMI–Sentinel-5 Precursor formaldehyde validation using an extensive network of ground-based Fourier-transform infrared stations, Atmos. Meas. Tech., 13, 3751–3767, https://doi.org/10.5194/amt-13-3751-2020, 2020.

Wagner, T. J., Czarnetzki, A. C., Christiansen, M., Pierce, R. B., Stanier, C. O., Dickens, A. F., and Eloranta, E. W.: Observations of the development and vertical structure of the lake-breeze circulation during the 2017 Lake Michigan Ozone Study, J. Atmos. Sci., 79(4), 1005–1020, https://doi.org/10.1175/JAS-D-20-0297.1, 2022.

Zoogman, P., Liu, X., Suleiman, R. M., Pennington, W. F., Flittner, D. E., Al-Saadi, J. A., Hilton, B. B., Nicks, D. K., Newchurch, M. J., Carr, J. L., Janz, S. J., Andraschko, M. R., Arola, A., Baker, B. D., Canova, B. P., Chan Miller, C., Cohen, R. C., Davis, J. E., Dussault, M. E., Edwards, D. P., Fishman, J., Ghulam, A., González Abad, G., Grutter, M., Herman, J. R., Houck, J., Jacob, D. J., Joiner, J., Kerridge, B. J., Kim, J., Krotkov, N. A., Lamsal, L., Li, C., Lindfors, A., Martin, R. V.,

https://doi.org/10.5194/egusphere-2022-1154
Preprint. Discussion started: 9 December 2022

McElroy, C. T., McLinden, C., Natraj, V., Neil, D. O., Nowlan, C. R., O'Sullivan, E. J., Palmer, P. I., Pierce, R. B., Pippin, M. R., Saiz-Lopez, A., Spurr, R. J. D., Szykman, J. J., Torres, O., Veefkind, J. P., Veihelmann, B., Wang, H., Wang, J., and Chance, K.: Tropospheric emissions: Monitoring of pollution (TEMPO), J. Quant. Spectrosc. Radiat. Transfer, 186, 17–39, https://doi.org/10.1016/j.jqsrt.2016.05.008, 2017.